Supplementary material

Evaluation of stratospheric transport in three generations of Chemistry-Climate Models

This Supplementary material presents additional figures, analogous to those in the main document but showing the individual behavior for each model.

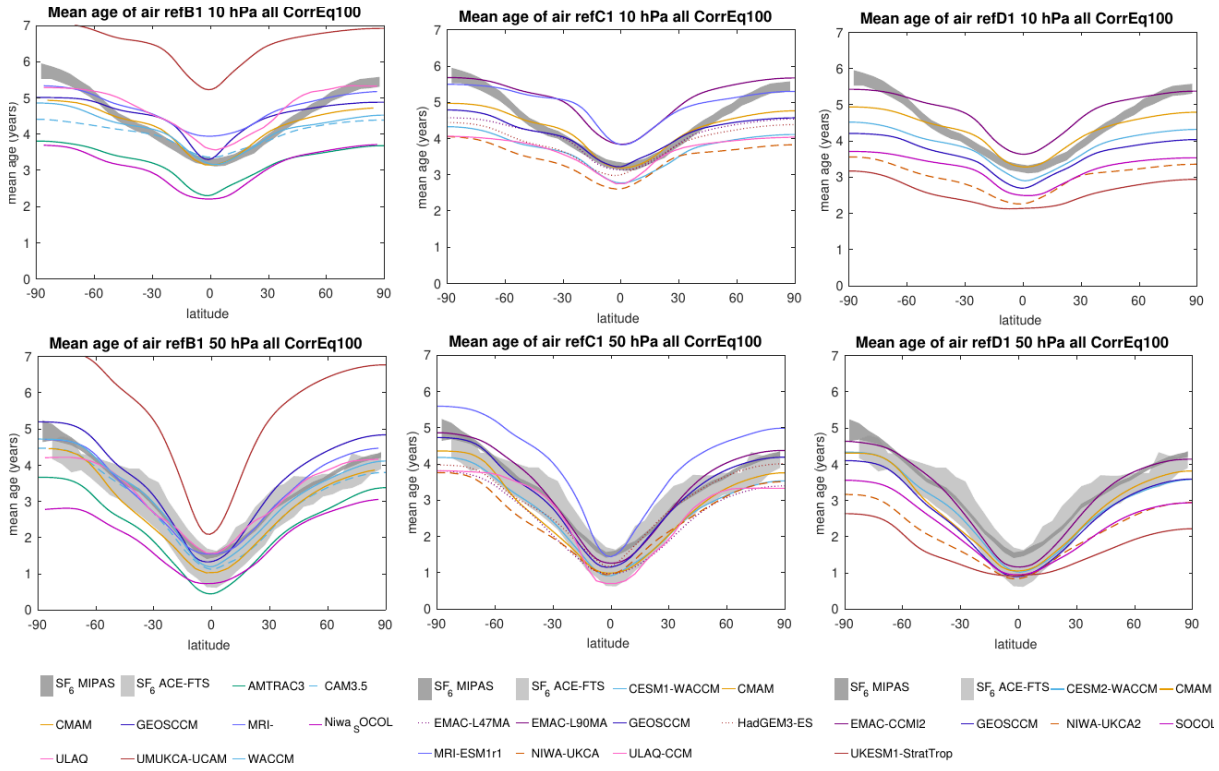

Figure 1S. Latitudinal structure of mean age of air in individual models participating in the three intercomparison initiatives (lines) and observational estimates (shading). Mean age values in each dataset are relative to the mean age at the equator and 100 hPa. Levels: 10 hPa (top row) and 50 hPa (bottom row).Time period considered for averages: 1990-2010 (1980-2000 for refB1).

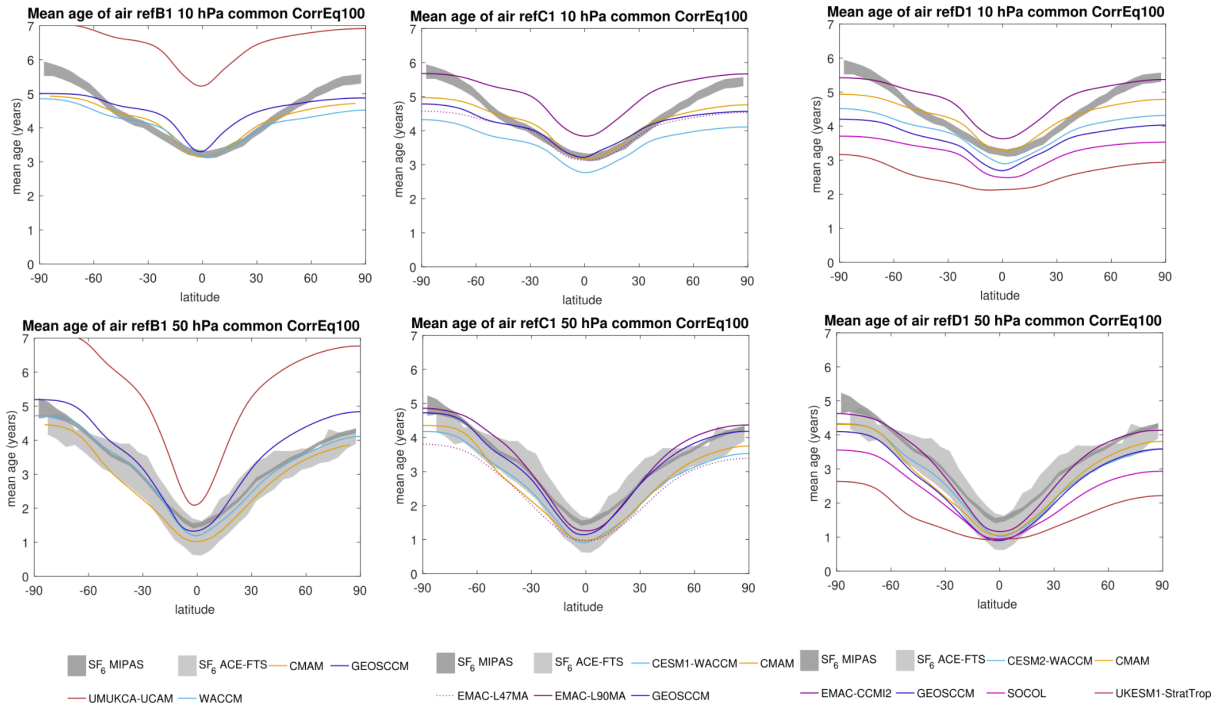

Figure 2S. As Fig. 1S but for common models only, that is, models in the eight families identified in Tables 1-3 of the main manuscript.

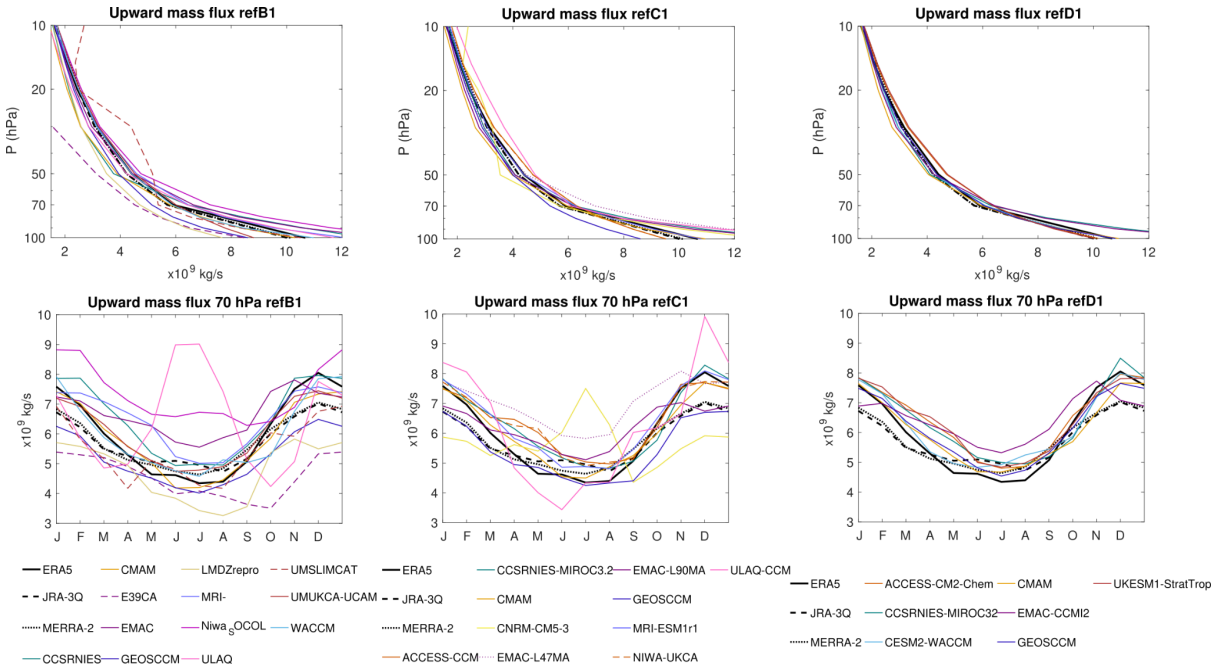

Figure 3S. Annual mean vertical profile (top row) and seasonal cycle at 70 hPa (bottom row) of upward mass flux in individual models participating in the three intercomparison initiatives and three reanalyses. Average period: 1990-2010 (1990-2000 for refB1).

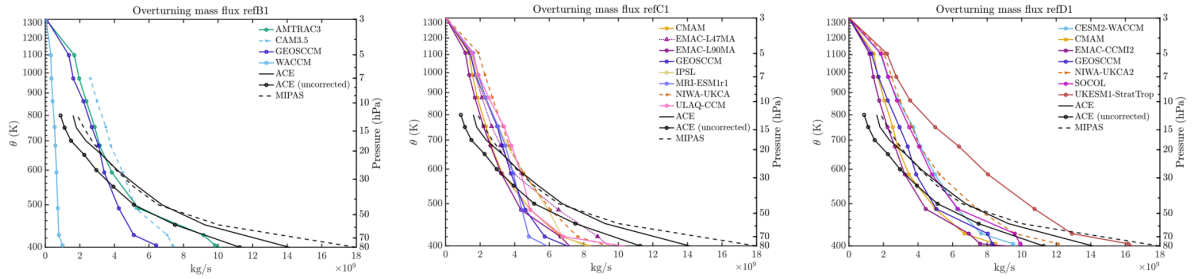

Figure 4S. Overturning mass flux from mean age of air meridional gradient for all individual models participating in the three intercomparison initiatives.

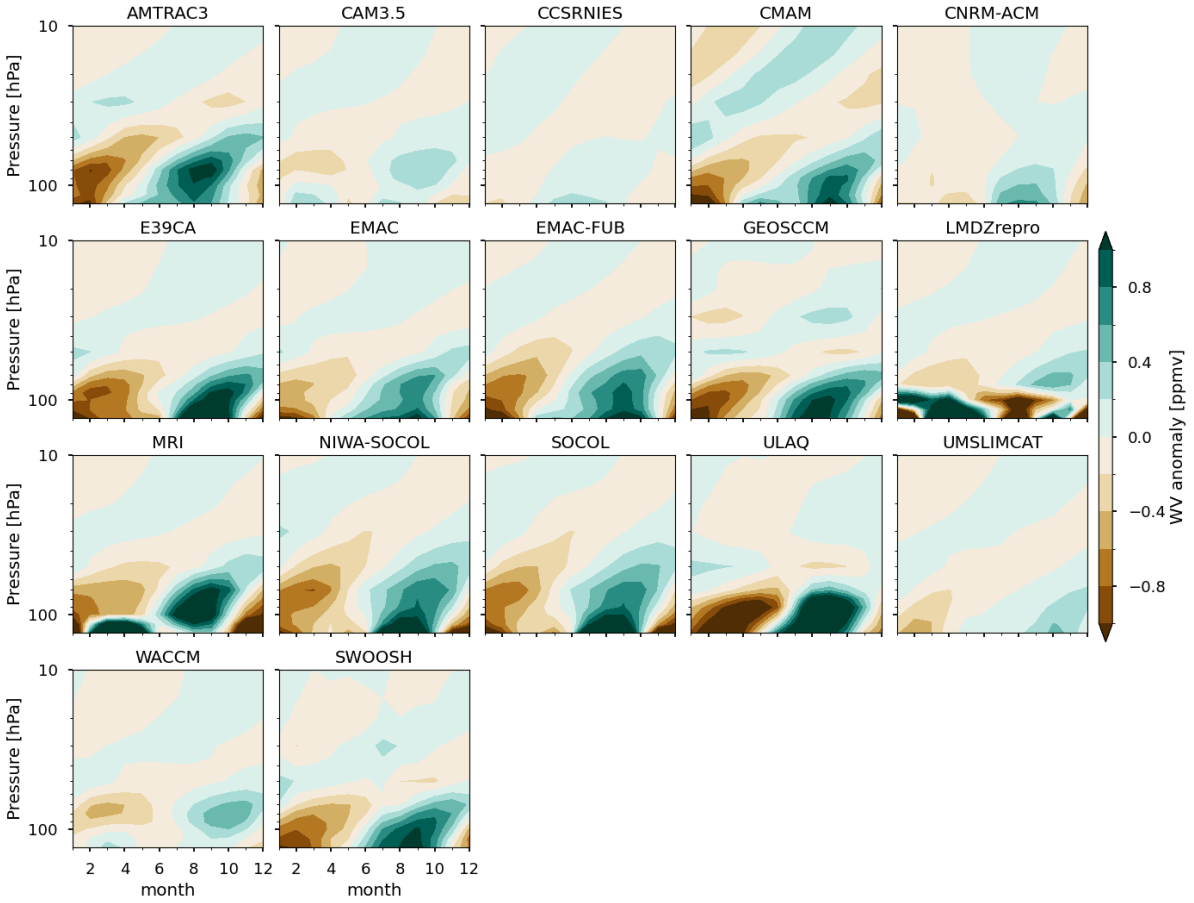

Figure 5S. Plots show the water vapor tape recorder anomalies for each refB1 model and SWOOSH (lower- and right-most panel). The anomaly is defined as the departure from the annual climatological mean value at each level. The climatological base period for all datasets is 1992 - 2005.

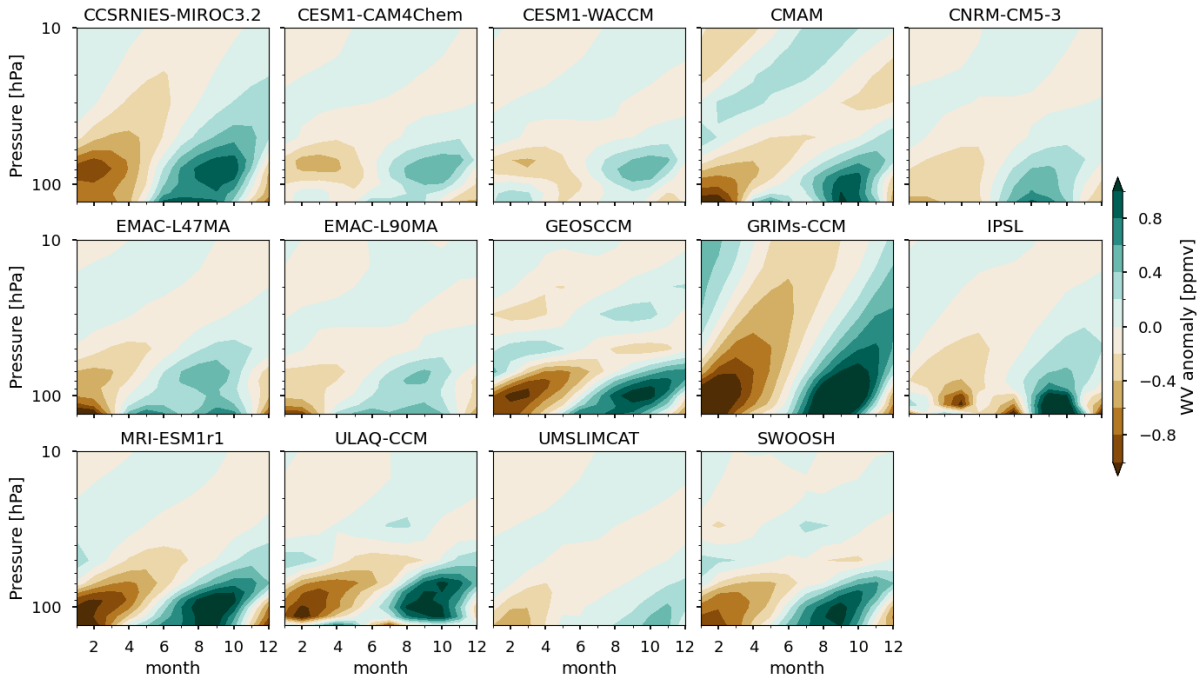

Fig. 6S. As Fig. 5S, but for refC1 using a 2005-2012 base period.

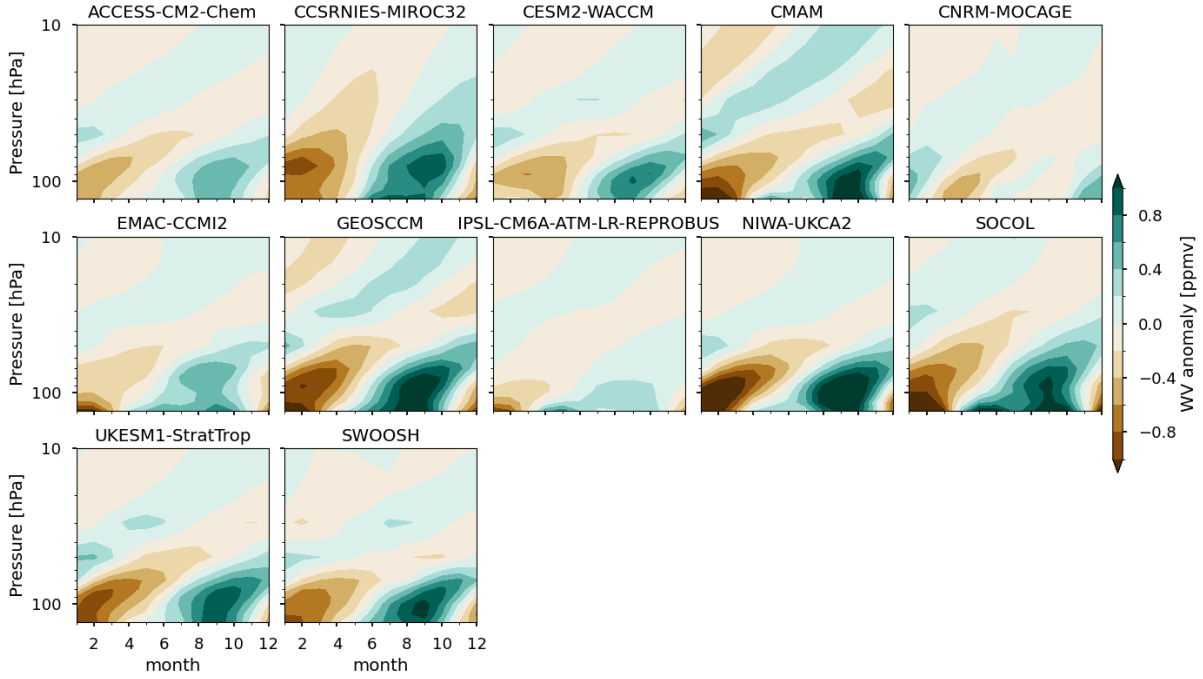

Figure 7S. Same as Fig. 5S, but for refD1 models using a 2005 - 2018 base period.

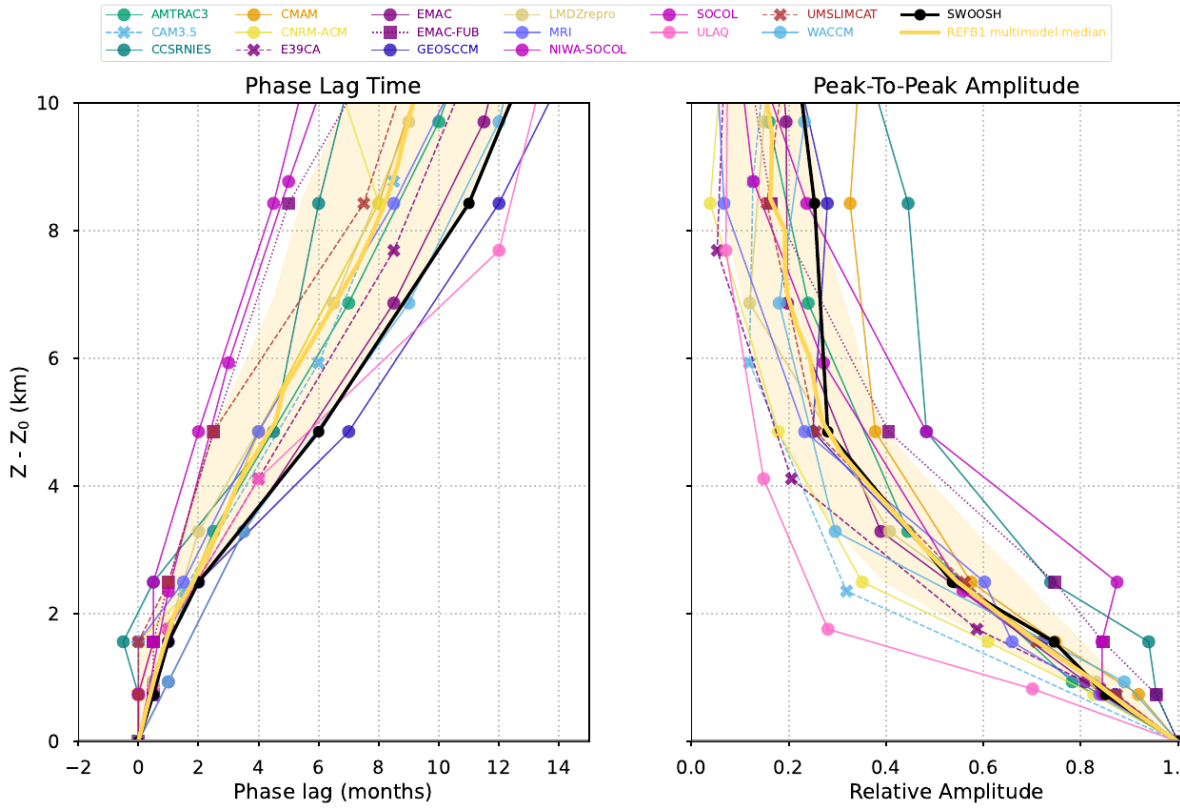
AMTRAC3
CAM3.5
CCSRNIES
CMAM
CNRM-ACM
E39CA
EMAC
EMAC-FUB
GEOSCCM
LMDZrepro
MRI
NIWA-SOCOL
SOCOL
ULAQ
UMSLIMCAT
WACCM
SWOOSH
REFB1 multimodel median
Phase Lag Time
Peak-To-Peak Amplitude
Z - Z0 (km)
Phase lag (months)
Relative Amplitude

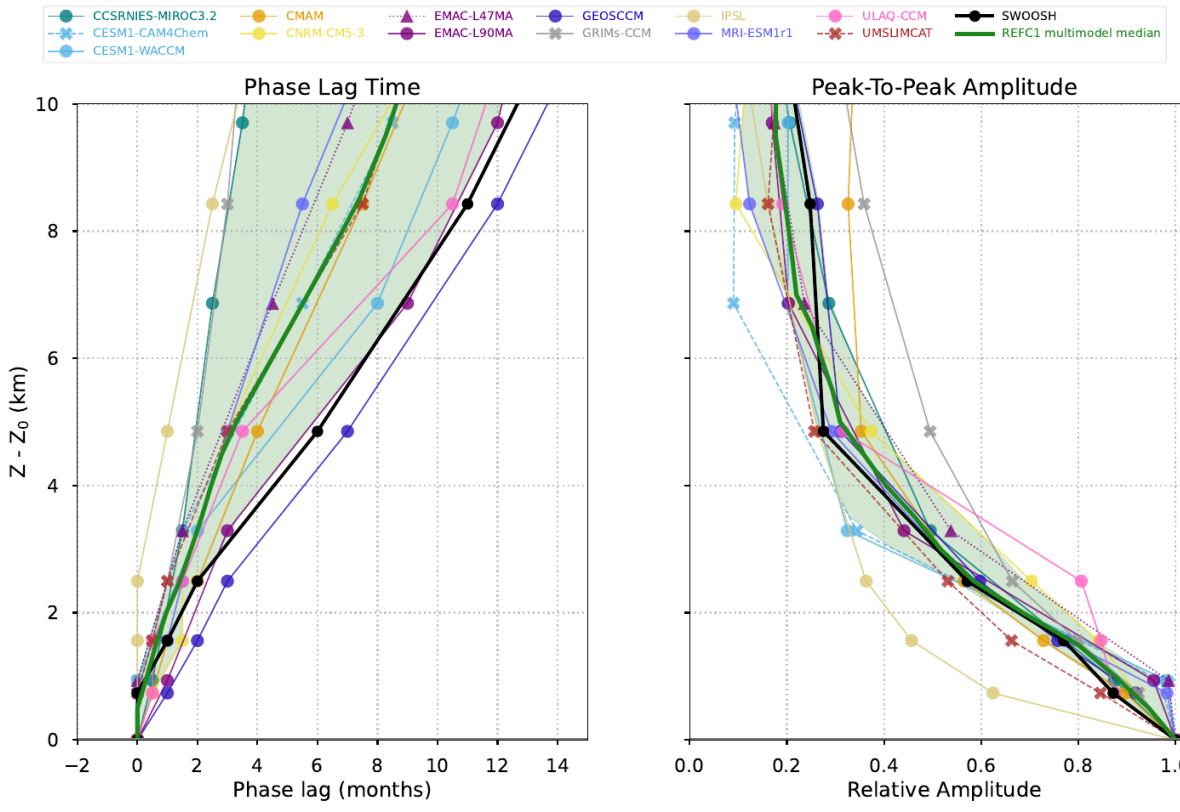
CCSRNIES-MIROC3.2
CESM1-CAM4Chem
CESM1-WACCM
CMAM
CNRM-CM5-3
EMAC-L47MA
EMAC-L90MA
GEOSCCM
GRIMs-CCM
IPSL
MRI-ESM1r1
ULAQ-CCM
UMSLIMCAT
SWOOSH
REFC1 multimodel median
Phase Lag Time
Peak-To-Peak Amplitude
Z - Z0 (km)
Phase lag (months)
Relative Amplitude

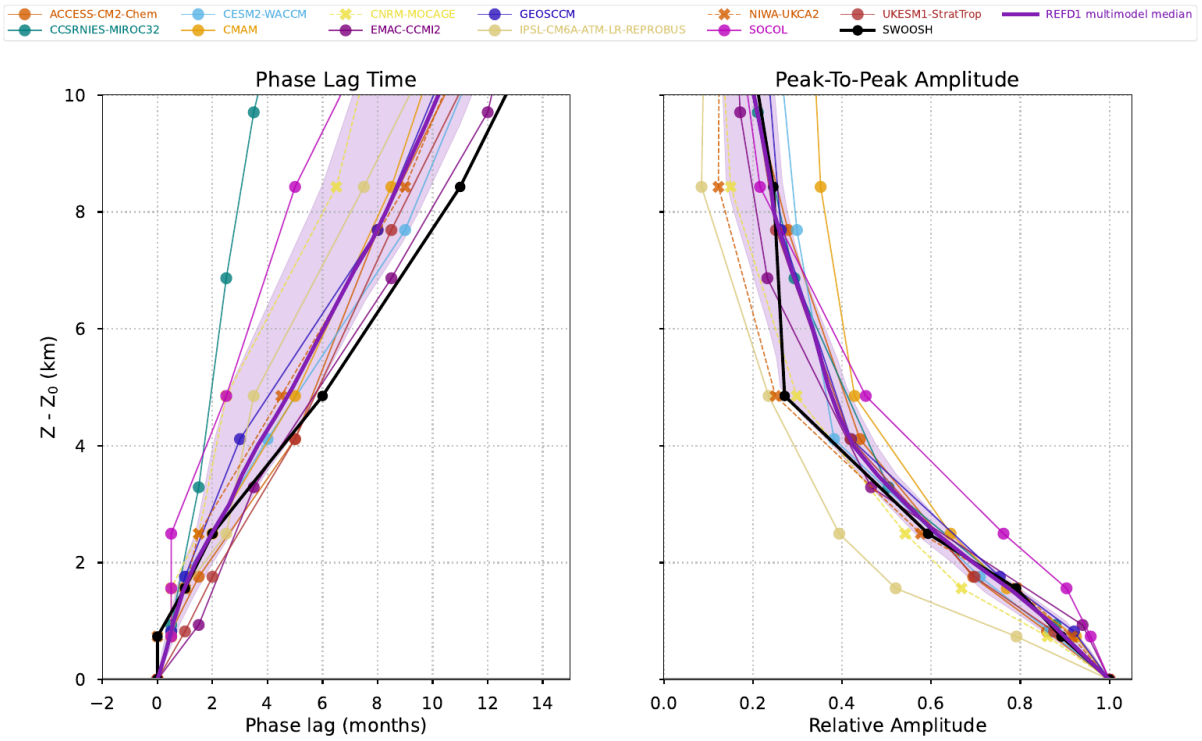

Figure 8S. Phase and amplitude of tape recorder signal as a function of tropopause-relative altitude for individual models participating in the three intercomparison initiatives and the SWOOSH dataset.

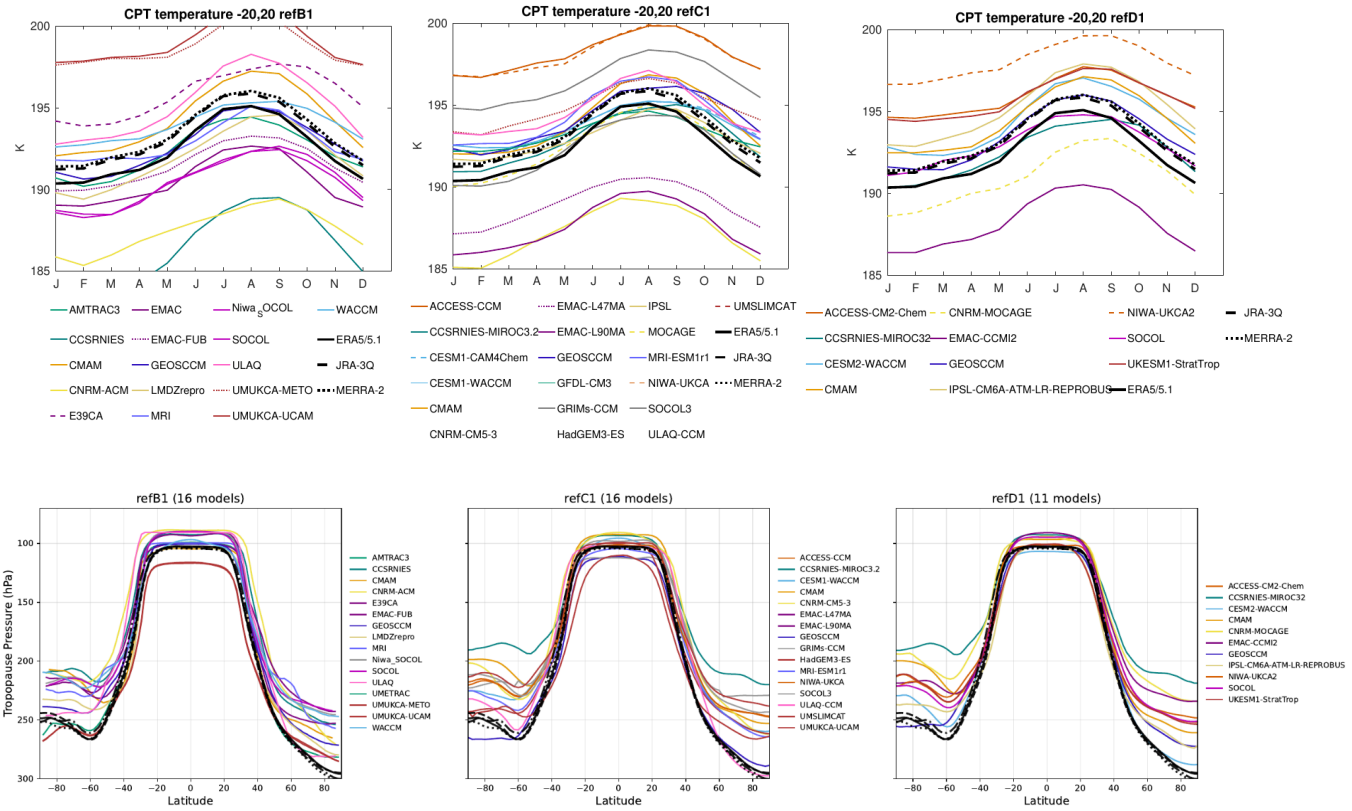

Figure 9S. Cold-point tropopause temperature seasonal cycle (top panels) and annual mean lapse rate tropopause pressure as a function of latitude (bottom panels) for individual models participating in the three intercomparison initiatives and three reanalyses.

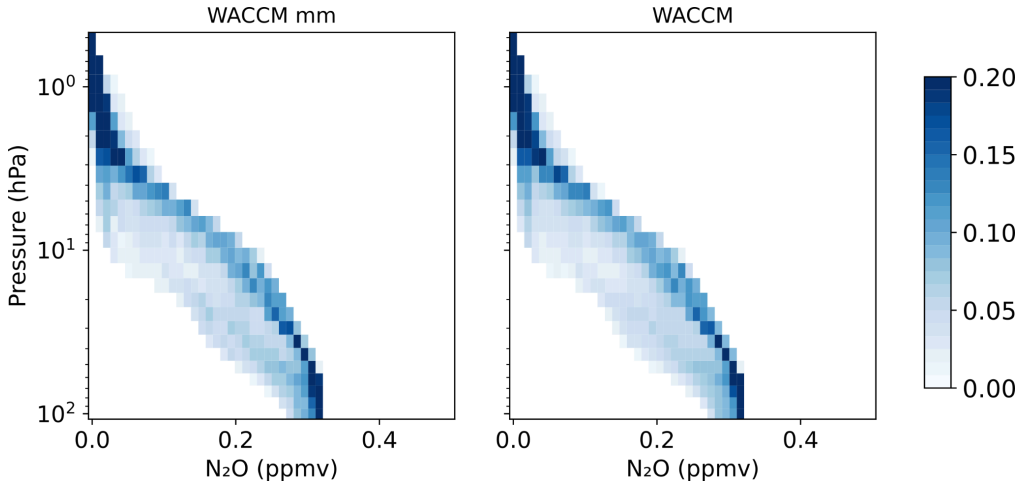

Figure 10S. N2O PDF for CESM1-WACCM using daily mean (right panel) versus monthly mean (left) output.

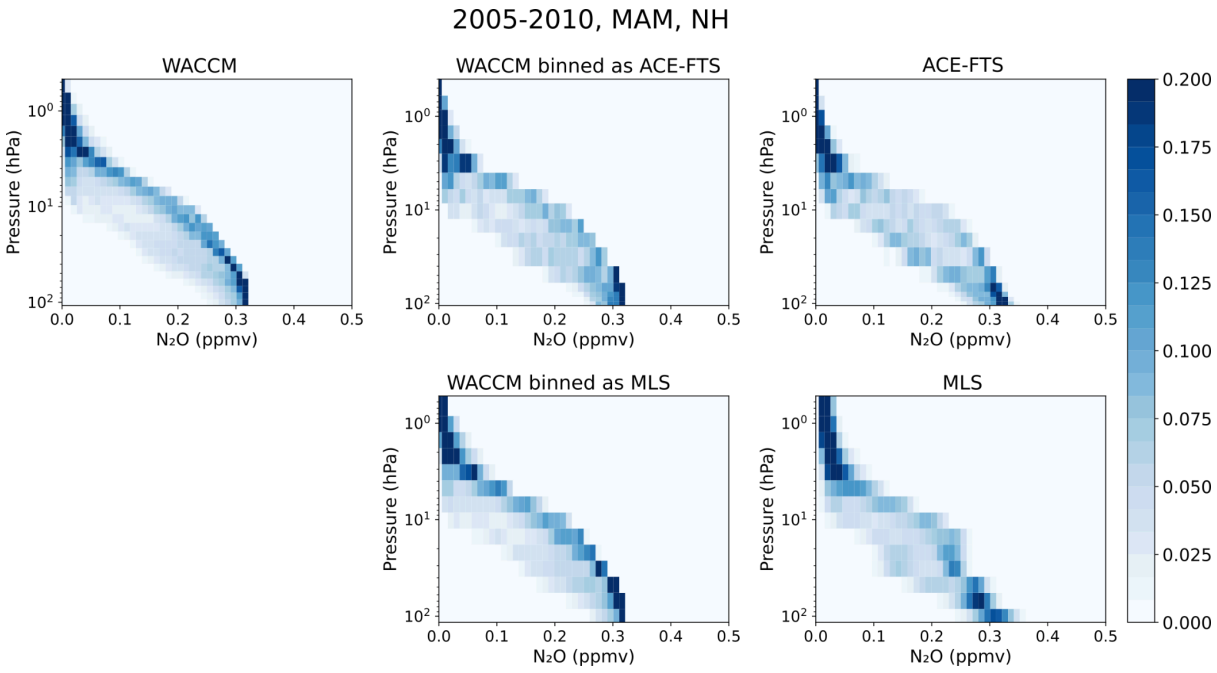

Figure 11S. N2O PDF for CESM1-WACCM using daily mean output with all spatial points (left panel) versus subsampling the model with the satellite trajectory for ACE-FTS (middle top panel) and MLS (middle bottom panel). The results for each satellite are shown in the right panels for comparison.

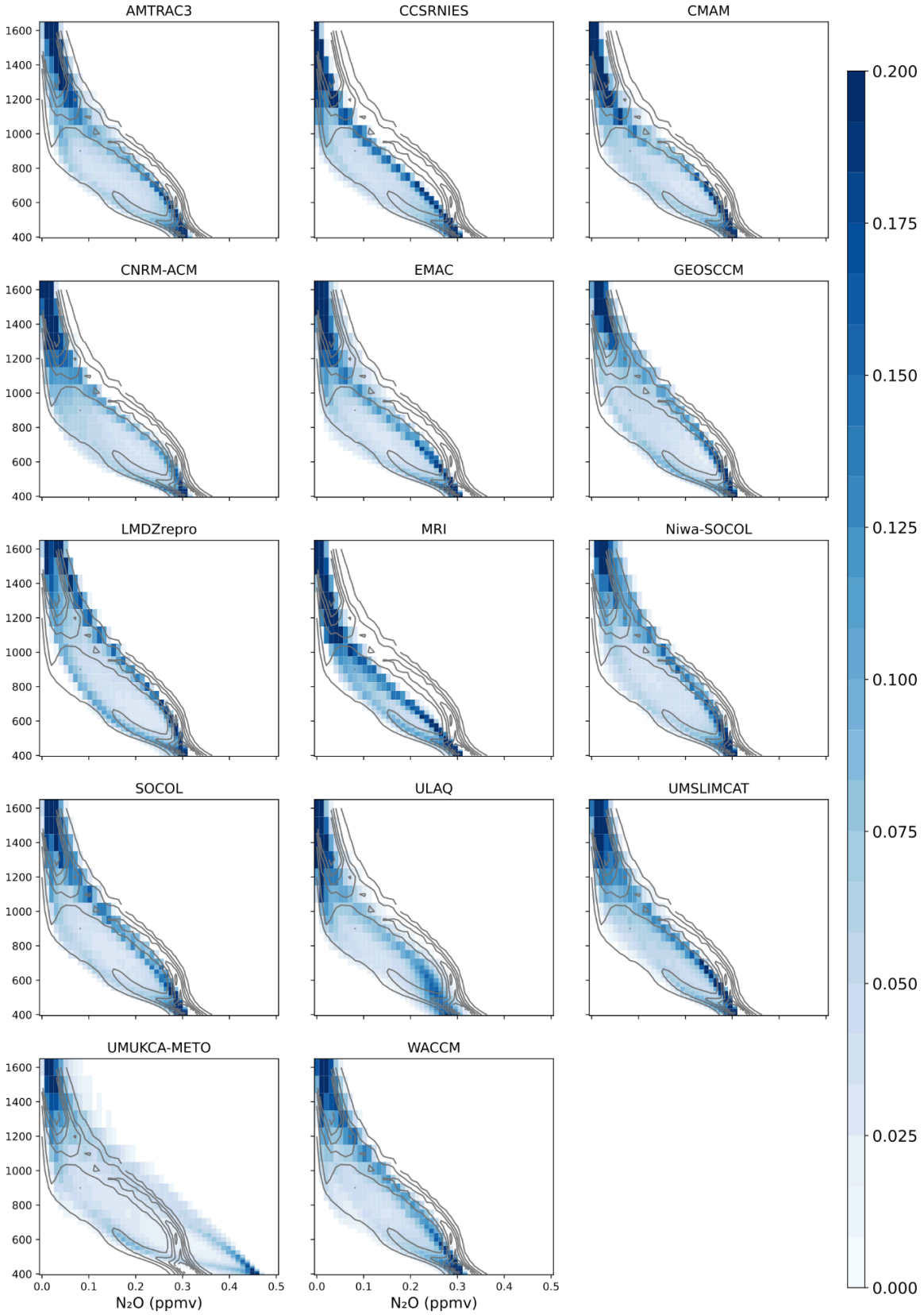

Figure 12S. N2O PDF in NH spring (MAM) for individual refB1 models.

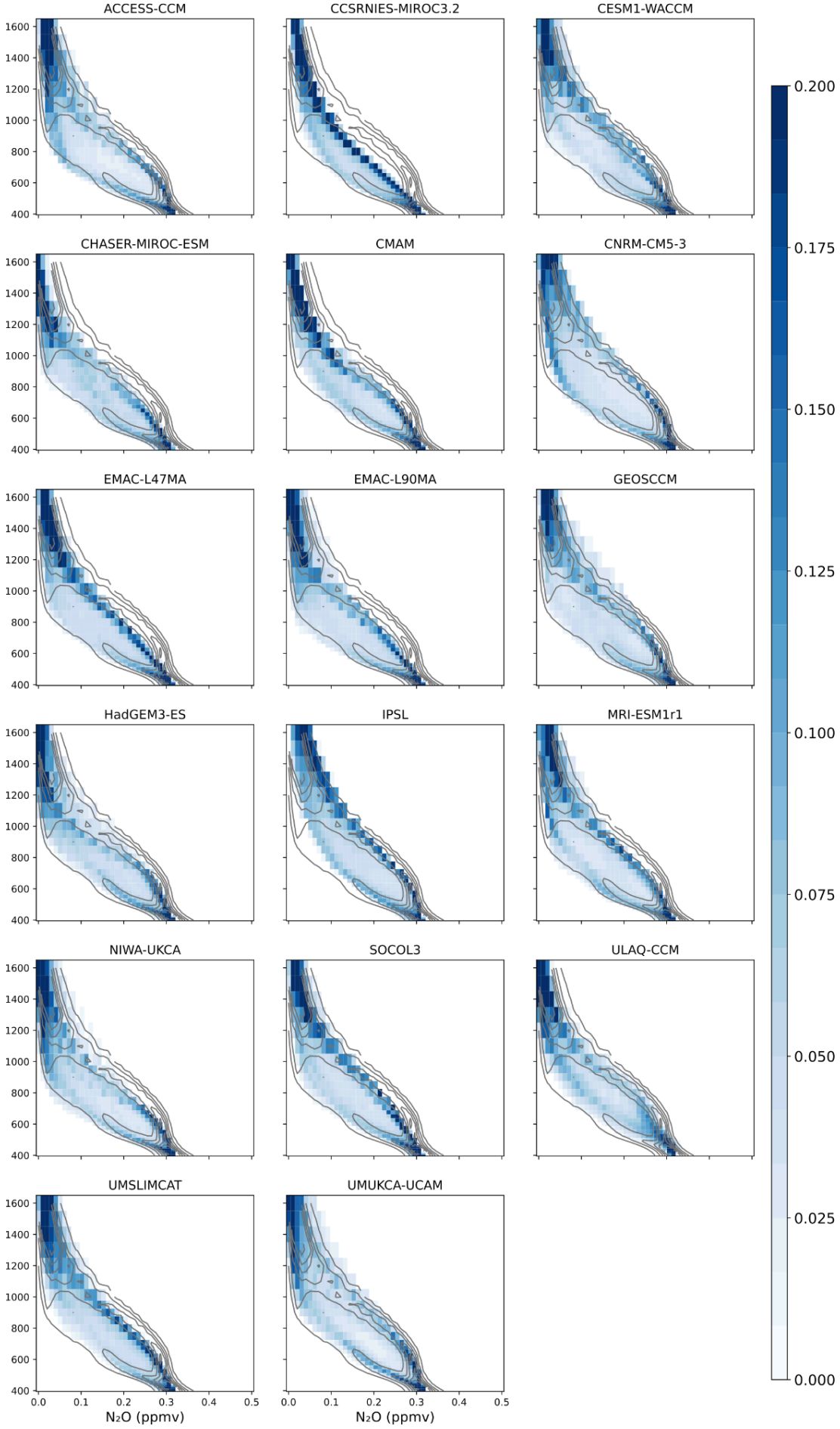
ACCESS-CCM
CCSRNIES-MIROC3.2
CESM1-WACCM
CHASER-MIROC-ESM
CMAM
CNRM-CM5-3
EMAC-L47MA
EMAC-L90MA
GEOSCCM
HadGEM3-ES
IPSL
MRI-ESM1r1
NIWA-UKCA
SOCOL3
ULAQ-CCM
UMSLIMCAT
UMUKCA-UCAM
1600
1400
1200
1000
800
600
400
0.0
0.1
0.2
0.3
0.4
0.5
N₂O (ppmv)
0.200
0.175
0.150
0.125
0.100
0.075
0.050
0.025
0.000

Figure 13S. N2O PDF in NH spring (MAM) for individual refC1 models.

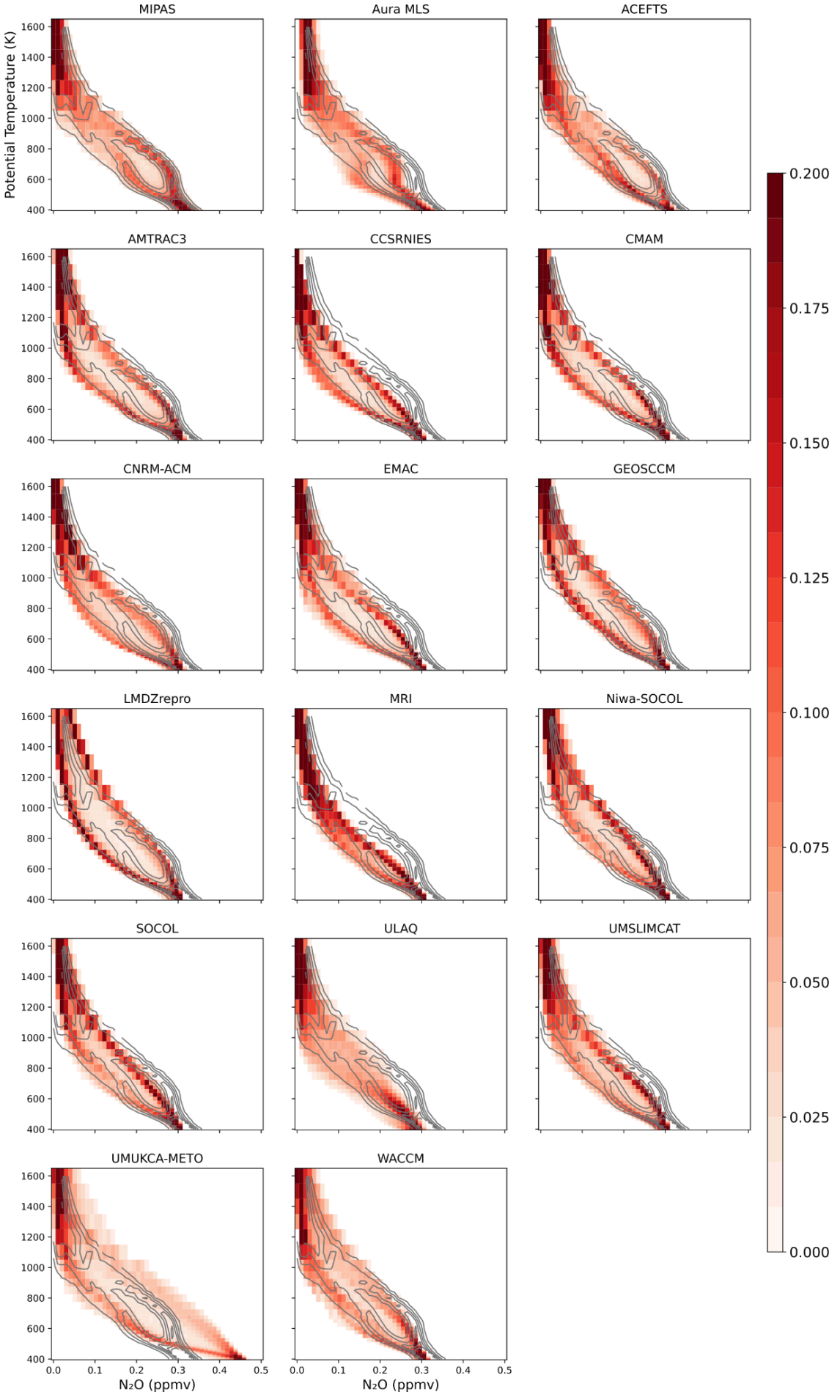
MIPAS
Aura MLS
ACEFTS
AMTRAC3
CCSRNIES
CMAM
CNRM-ACM
EMAC
GEOSCCM
LMDZrepro
MRI
Niwa-SOCOL
SOCOL
ULAQ
UMSLIMCAT
UMUKCA-METO
WACCM
Potential Temperature (K)
1600
1400
1200
1000
800
600
400
0.0
0.1
0.2
0.3
0.4
0.5
N₂O (ppmv)
0.200
0.175
0.150
0.125
0.100
0.075
0.050
0.025
0.000

Figure 14S. N2O PDF in SH spring (SON) for individual refB1 models.

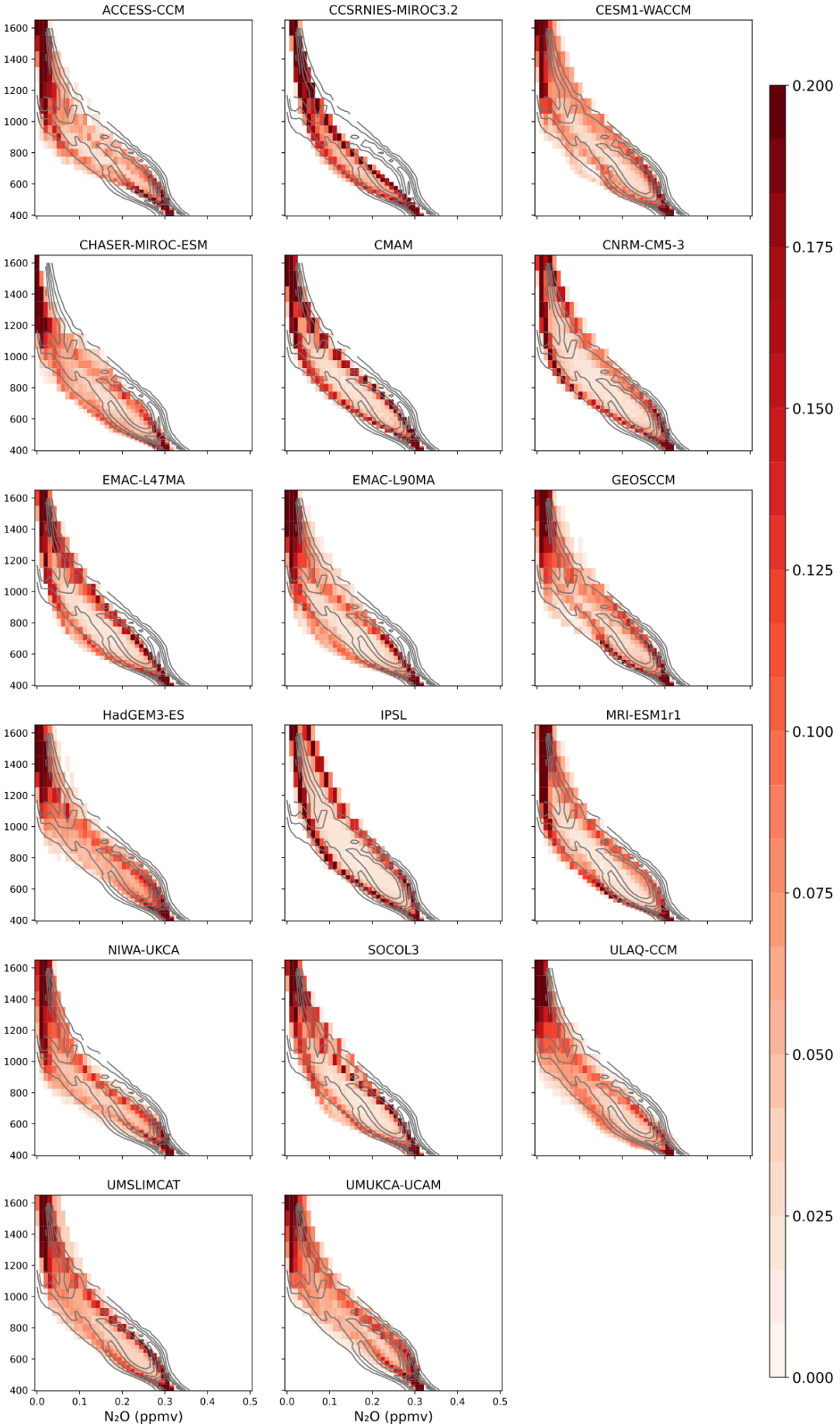
ACCESS-CCM
CCSRNIES-MIROC3.2
CESM1-WACCM
CHASER-MIROC-ESM
CMAM
CNRM-CM5-3
EMAC-L47MA
EMAC-L90MA
GEOSCCM
HadGEM3-ES
IPSL
MRI-ESM1r1
NIWA-UKCA
SOCOL3
ULAQ-CCM
UMSLIMCAT
UMUKCA-UCAM
1600
1400
1200
1000
800
600
400
0.0
0.1
0.2
0.3
0.4
0.5
N₂O (ppmv)
0.200
0.175
0.150
0.125
0.100
0.075
0.050
0.025
0.000

Figure 15S. N2O PDF in SH spring (SON) for individual refC1 models.

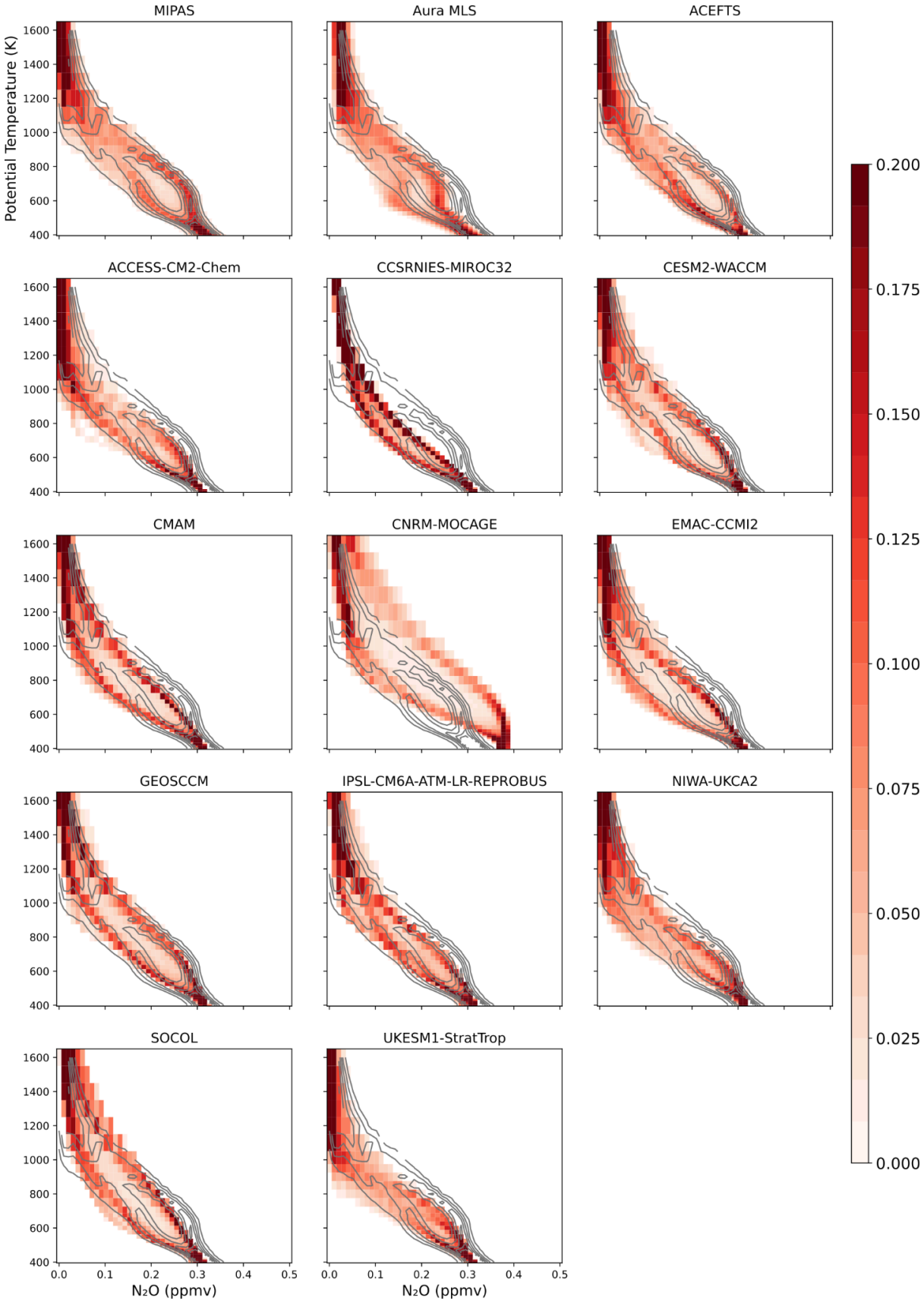

Figure 16S. N2O PDF in SH spring (SON) for individual refD1 models.

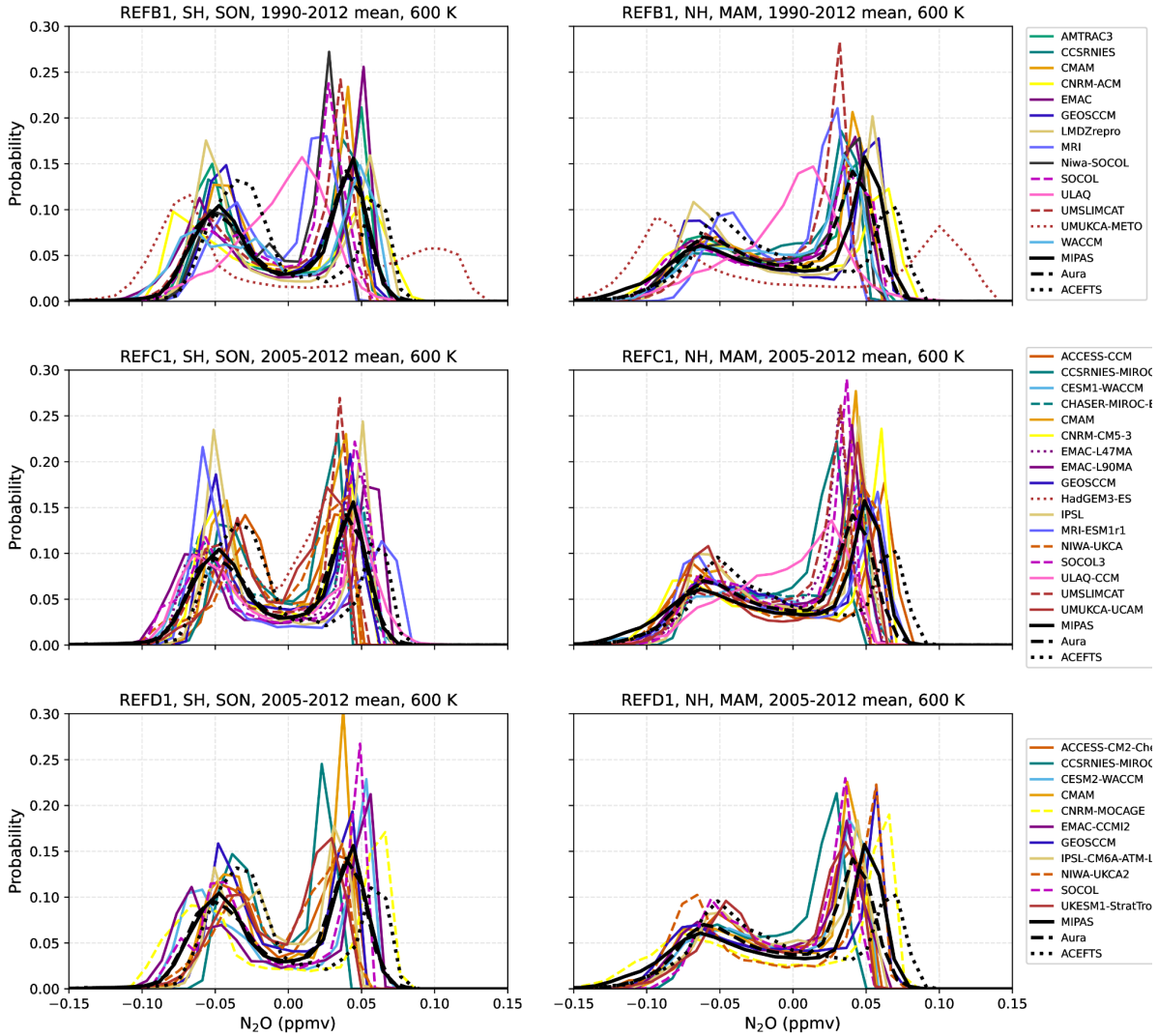

Figure 17S. N2O PDF at 600 K for all individual models participating in the three intercomparison initiatives.

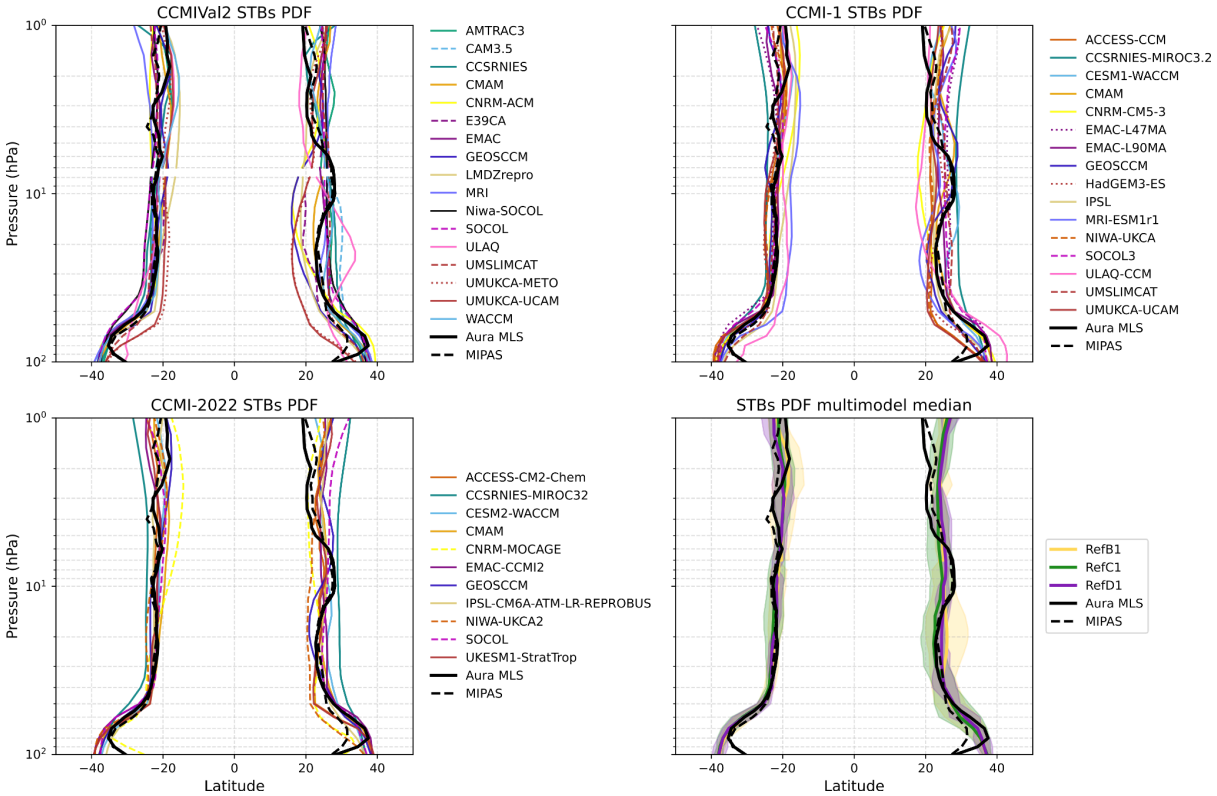

Figure 18S. Location of the annual mean subtropical mixing barriers (STBs) computed from the minimum in the N2O PDFs in individual models participating in the three intercomparison initiatives and for the multi-model median of each generation (right bottom panel).

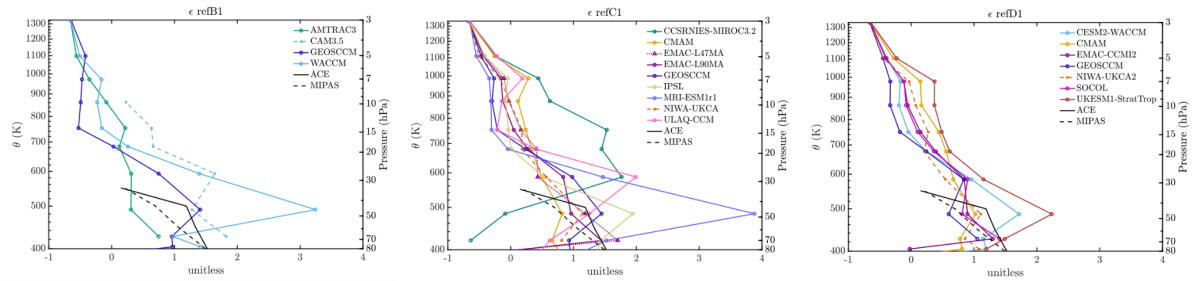

Figure 19S. Mixing efficiency calculations from age of air vertical gradient for individual models participating in the three initiatives.

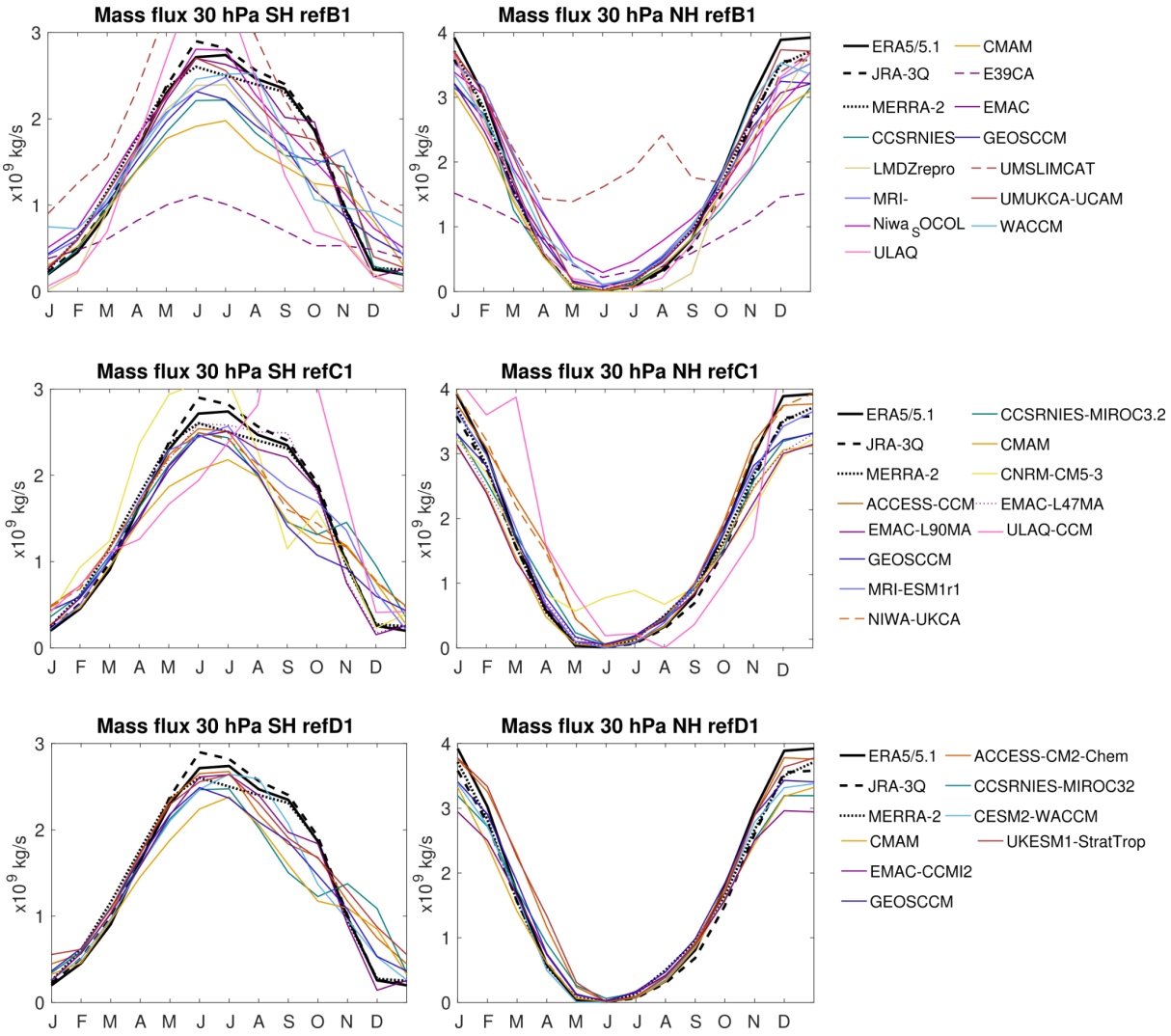

Figure 19S. Seasonal cycle of the downward mass flux in the SH (left) and NH (right) in individual models of the three intercomparison initiatives: refB1 (top), refC1 (middle) and refD1 (bottom) simulations.

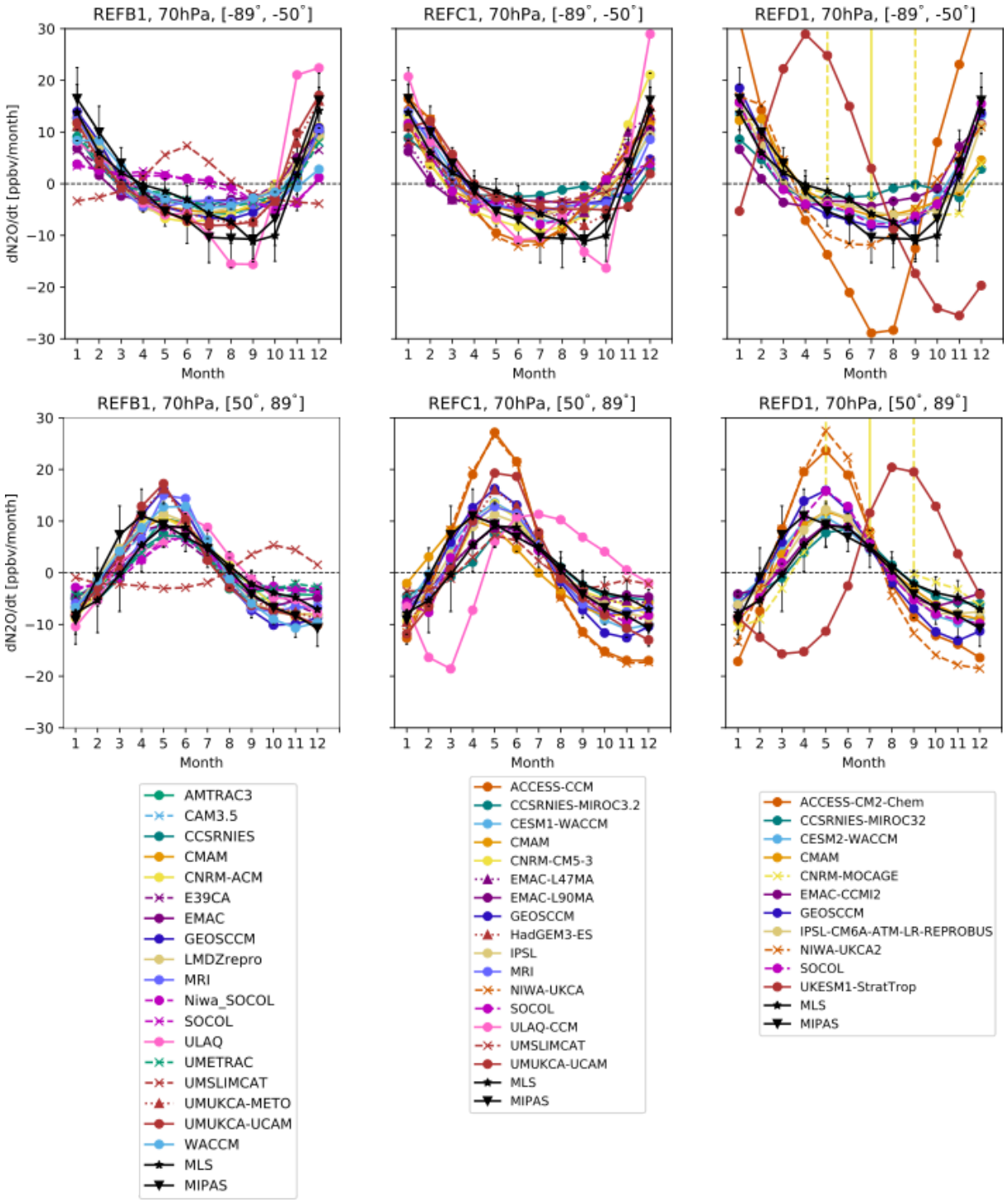

Figure 20S. Seasonal cycle of N2O monthly mean tendency in individual models participating in the three intercomparison initiatives and satellite datasets (top: SH, bottom: NH).

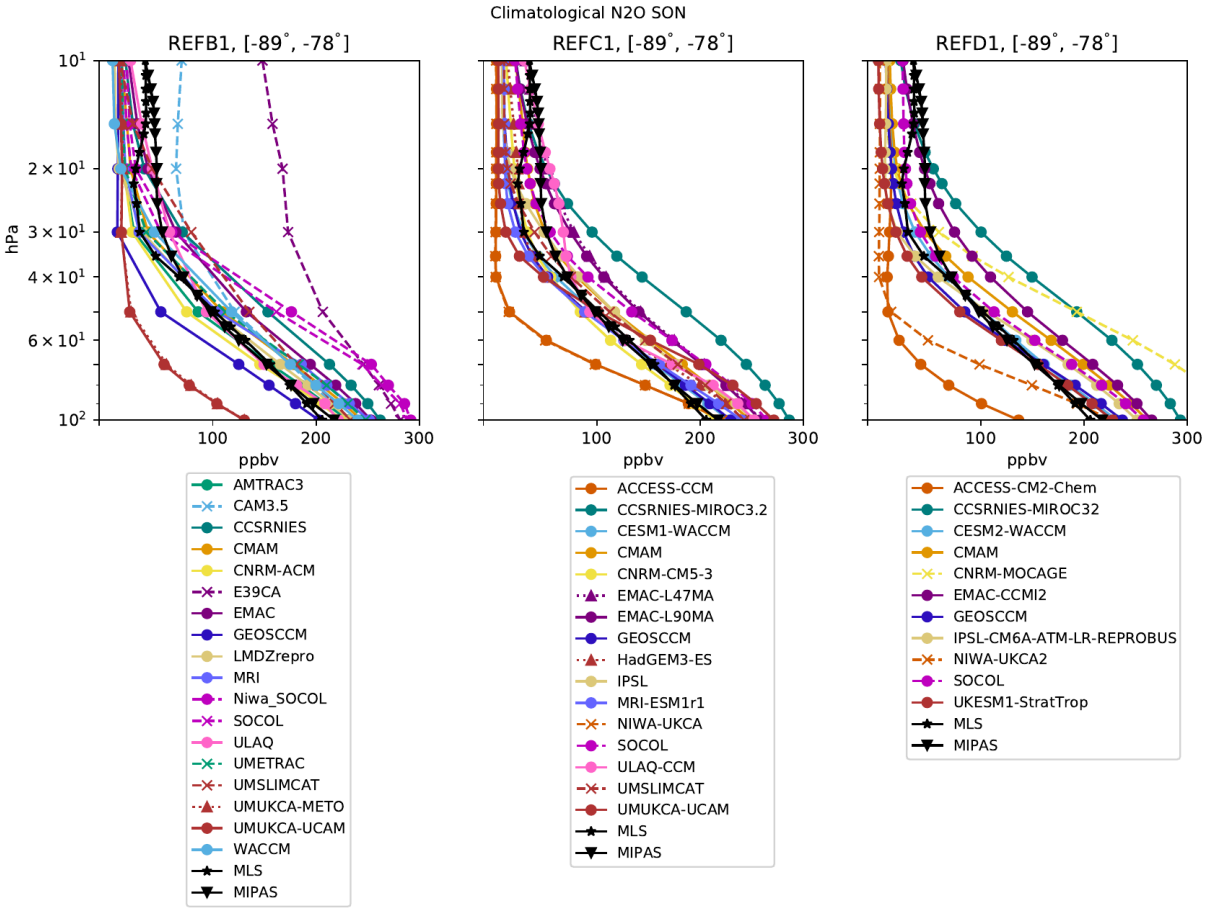

Figure 21S. Vertical profile of N2O for individual models participating in the three intercomparison initiatives and satellite datasets.

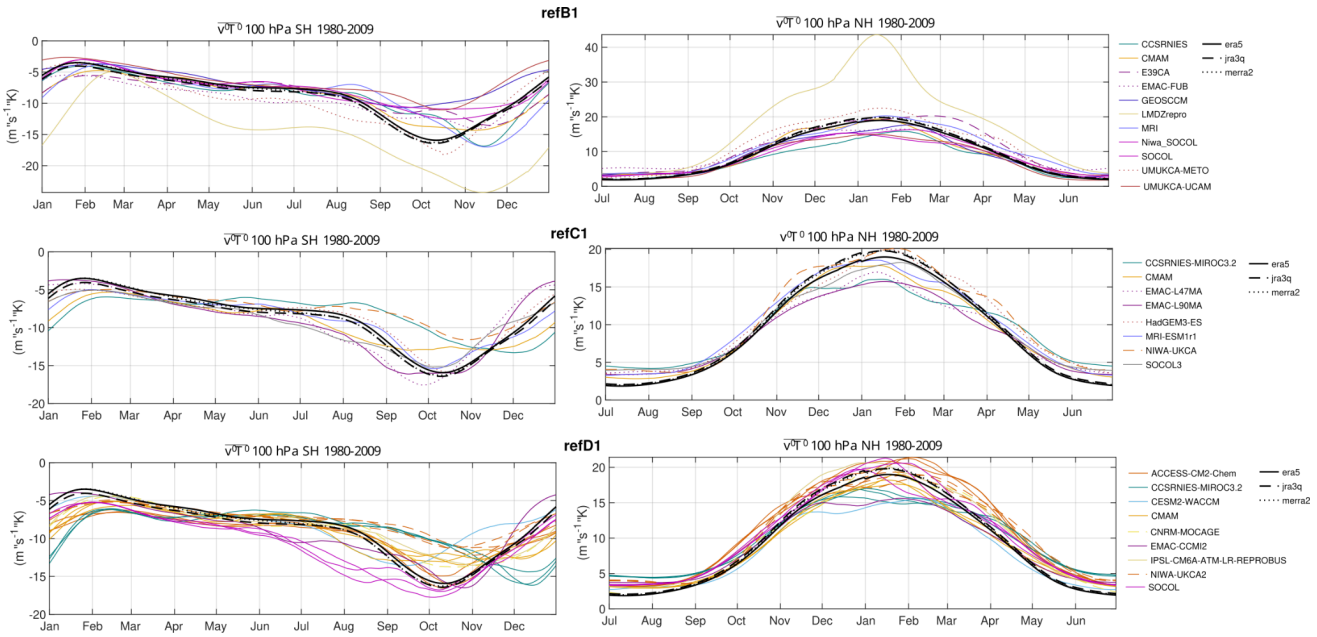

Figure 22S. Seasonal cycle of eddy heat flux in the NH (top panels) and SH (bottom panels) for the individual models participating in the three intercomparison initiatives (top.

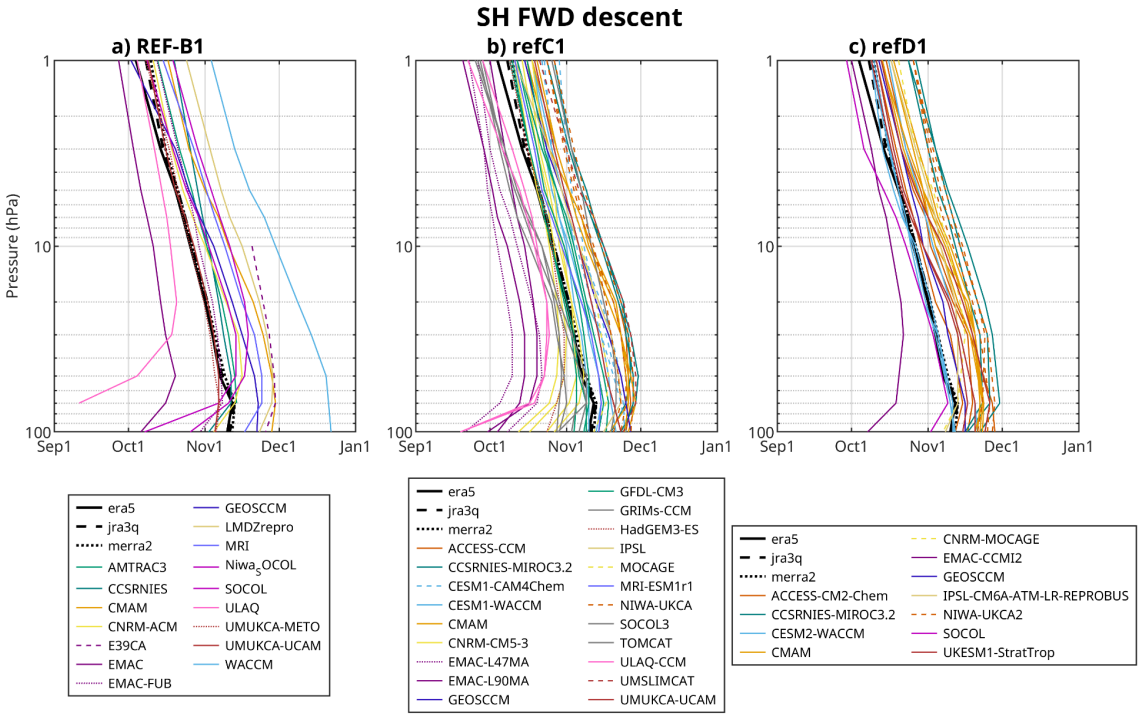

Figure 23S. Final warming descent date in the SH for individual models participating in the three intercomparison initiatives.

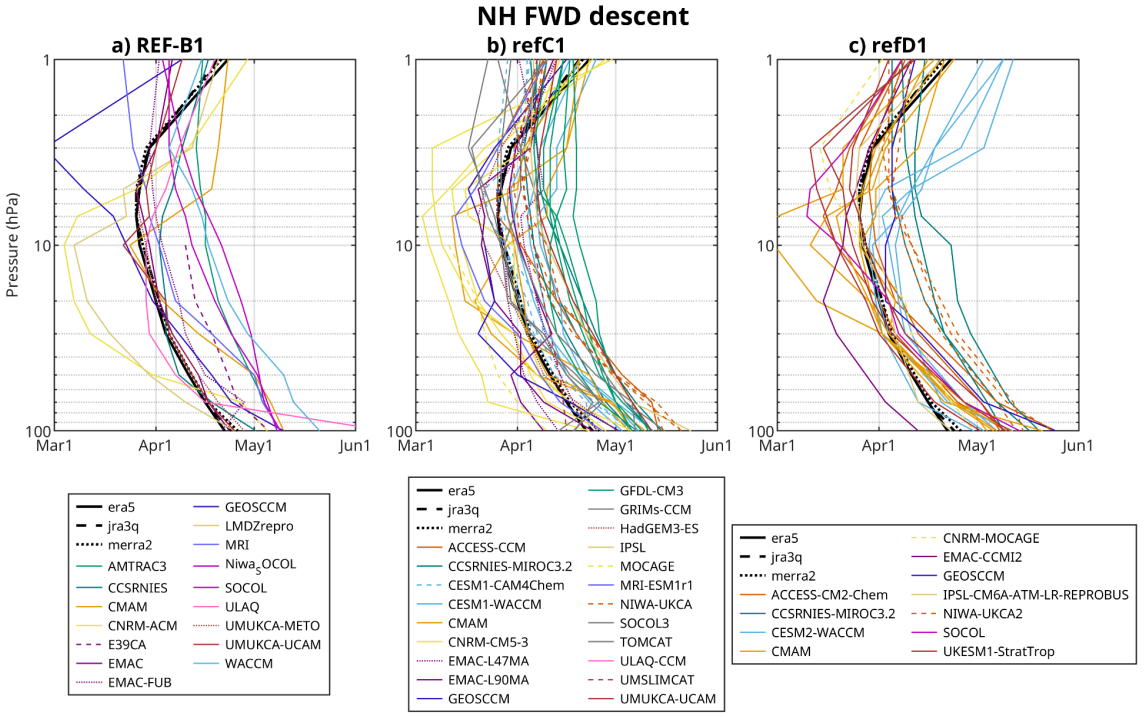

Figure 24S. Final warming descent date in the NH for individual models participating in the three intercomparison initiatives.

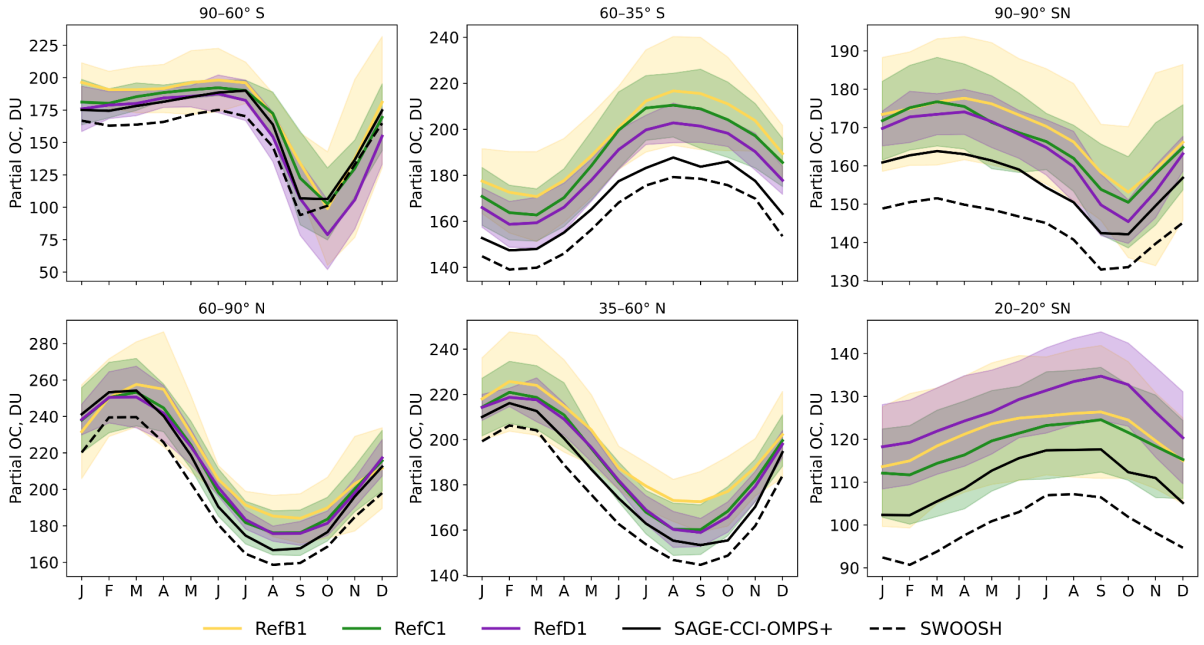

Figure 25S. Ozone partial column in the lower stratosphere for different latitude bands and global mean (top right panel). Multi-model mean and MAD computed using all available models (except clear outliers).

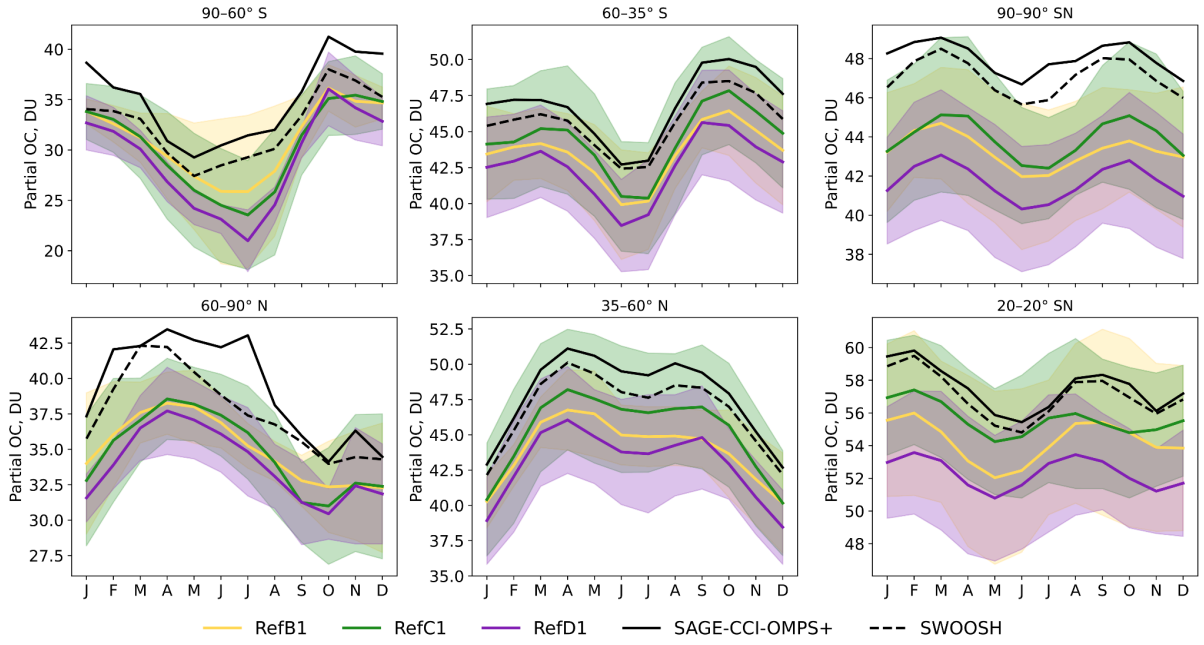

Figure 26S. Ozone partial column in the upper stratosphere for different latitude bands and global mean (top right panel). Multi-model mean and MAD computed using all available models (except clear outliers).

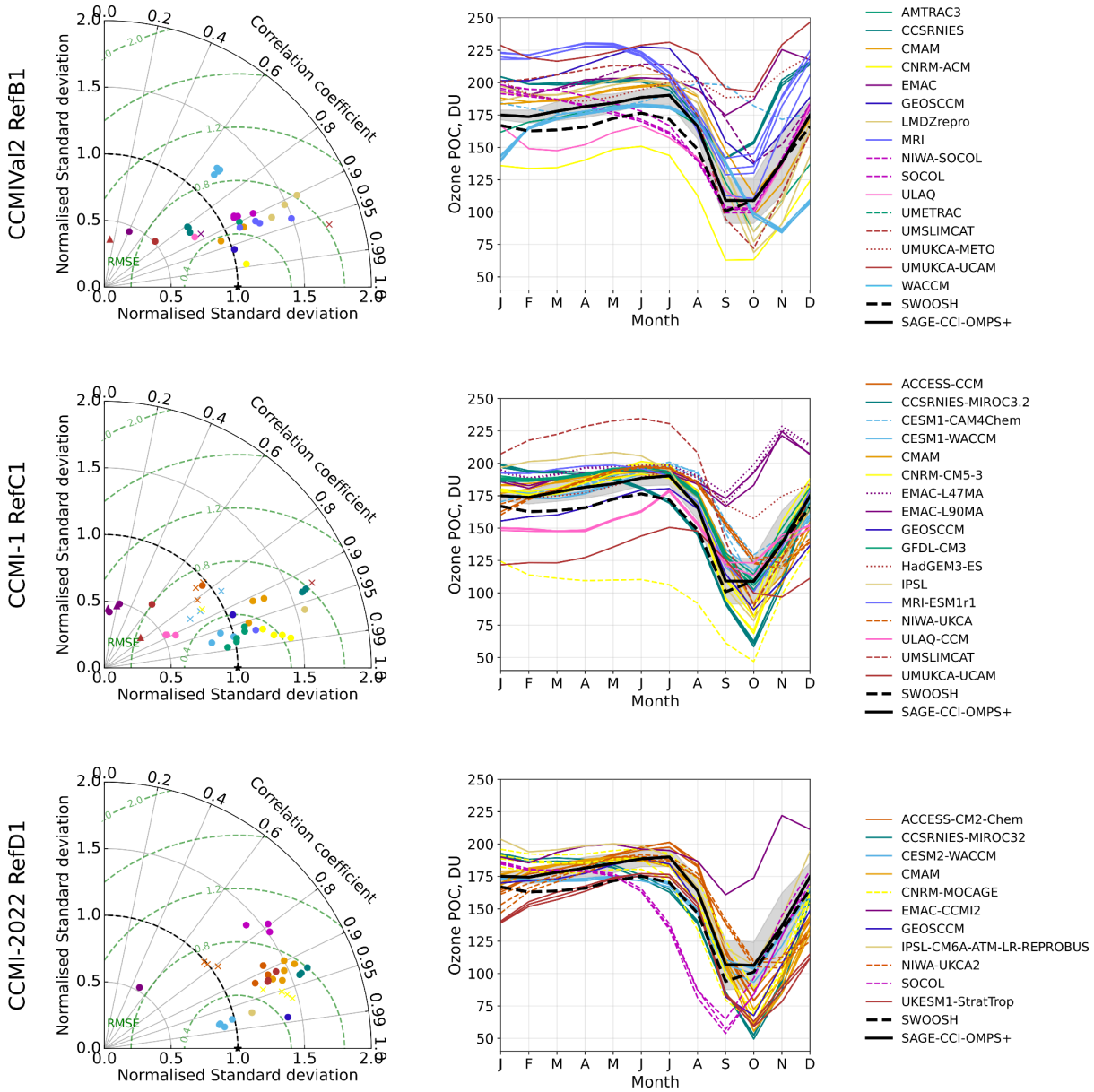

Figure 27S. Ozone partial column in the lower stratosphere for the SH polar region (90S-60S) for individual models participating in the three intercomparison initiatives. Left panels: Taylor diagrams. Right panels: seasonal cycle.

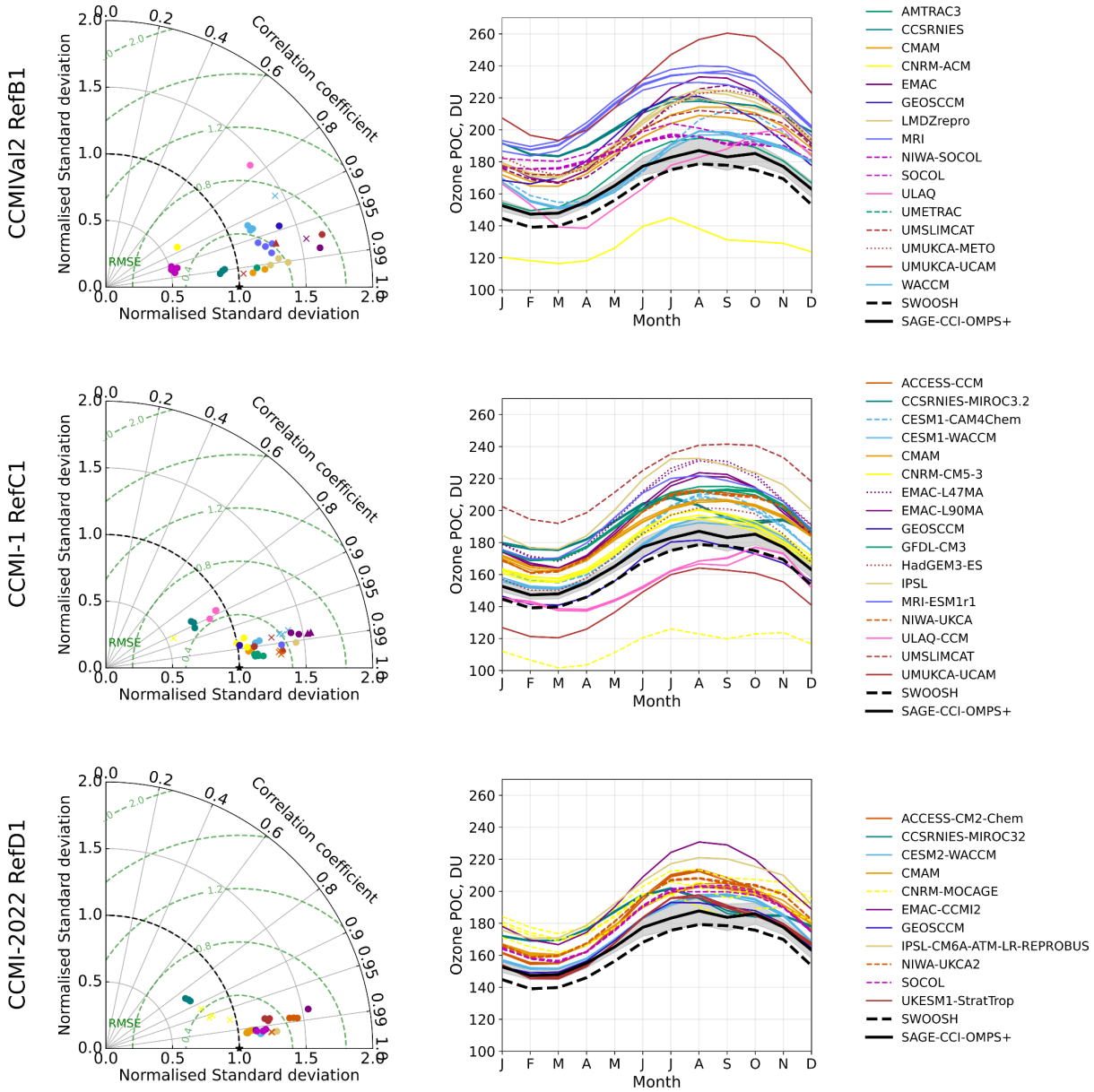

Figure 28S. Ozone partial column in the lower stratosphere for the SH midlatitudes region (60S-30S) for individual models participating in the three intercomparison initiatives. Left panels: Taylor diagrams. Right panels: seasonal cycle.

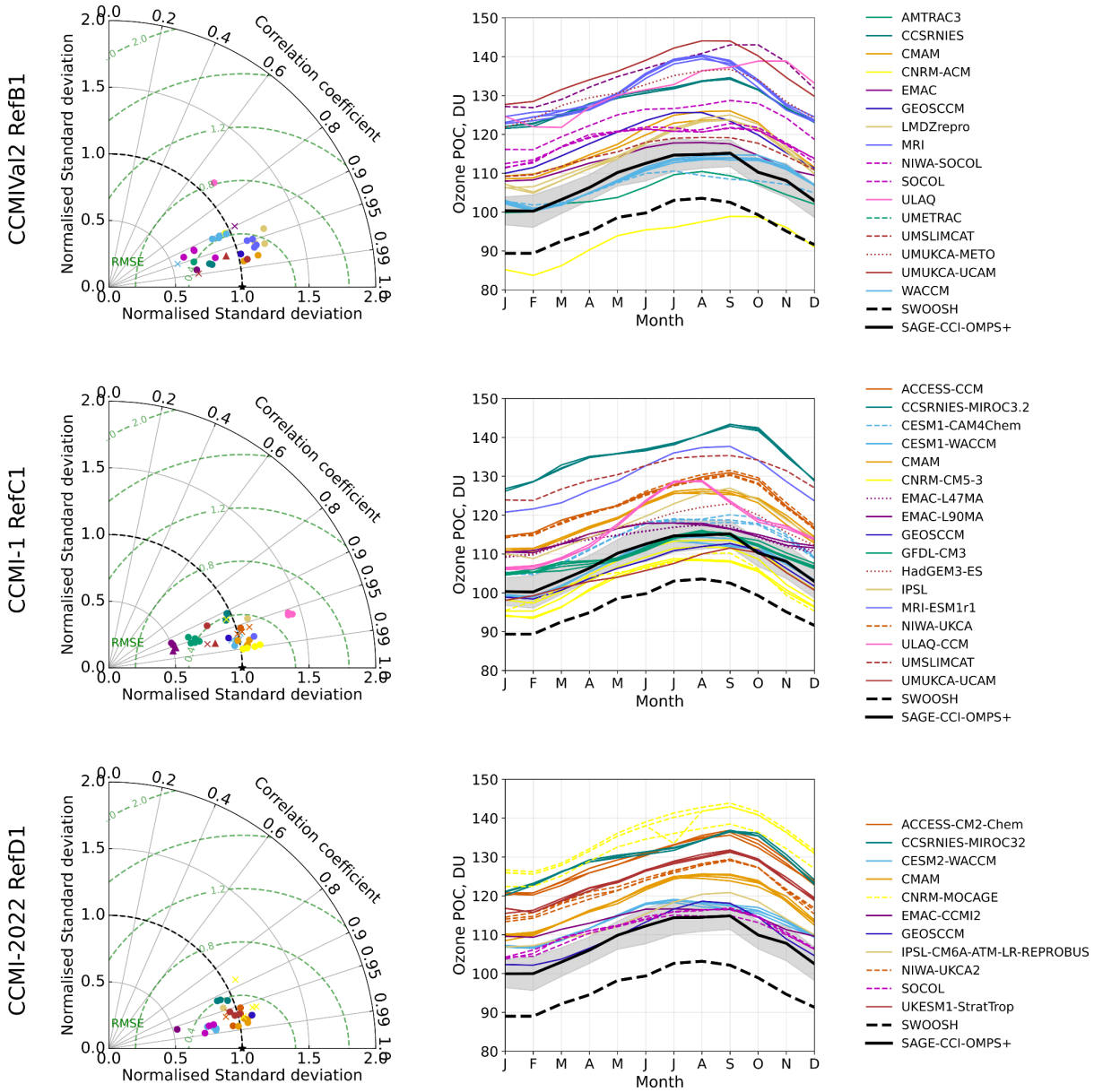

Figure 29S. Ozone partial column in the lower stratosphere for the tropics region (20S-20S) for individual models participating in the three intercomparison initiatives. Left panels: Taylor diagrams. Right panels: seasonal cycle.

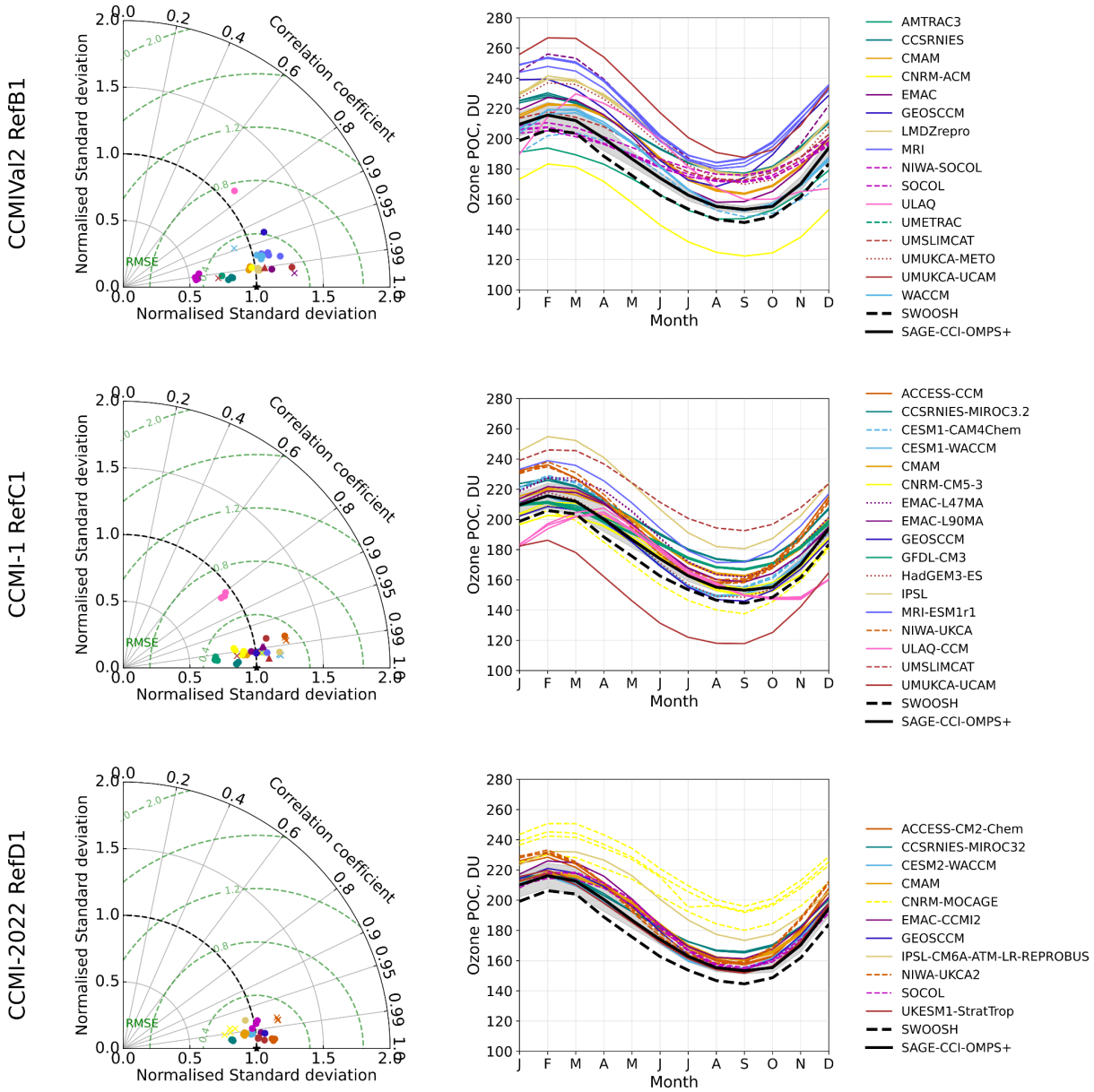

Figure 30S. Ozone partial column in the lower stratosphere for the NH midlatitudes region (30N-60N) for individual models participating in the three intercomparison initiatives. Left panels: Taylor diagrams. Right panels: seasonal cycle.

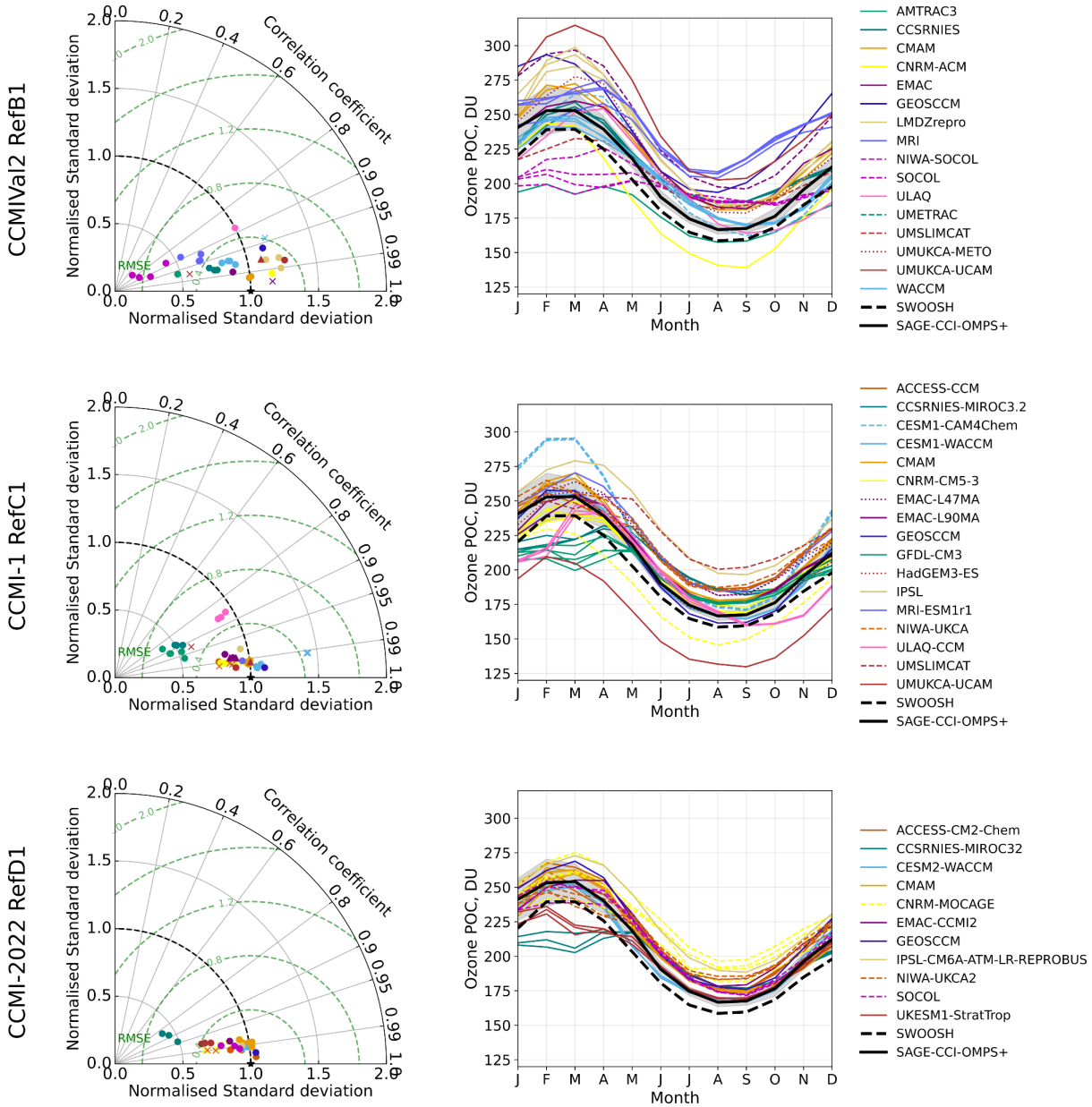

Figure 31S. Ozone partial column in the lower stratosphere for the NH polar region (60N-90N) for individual models participating in the three intercomparison initiatives. Left panels: Taylor diagrams. Right panels: seasonal cycle.

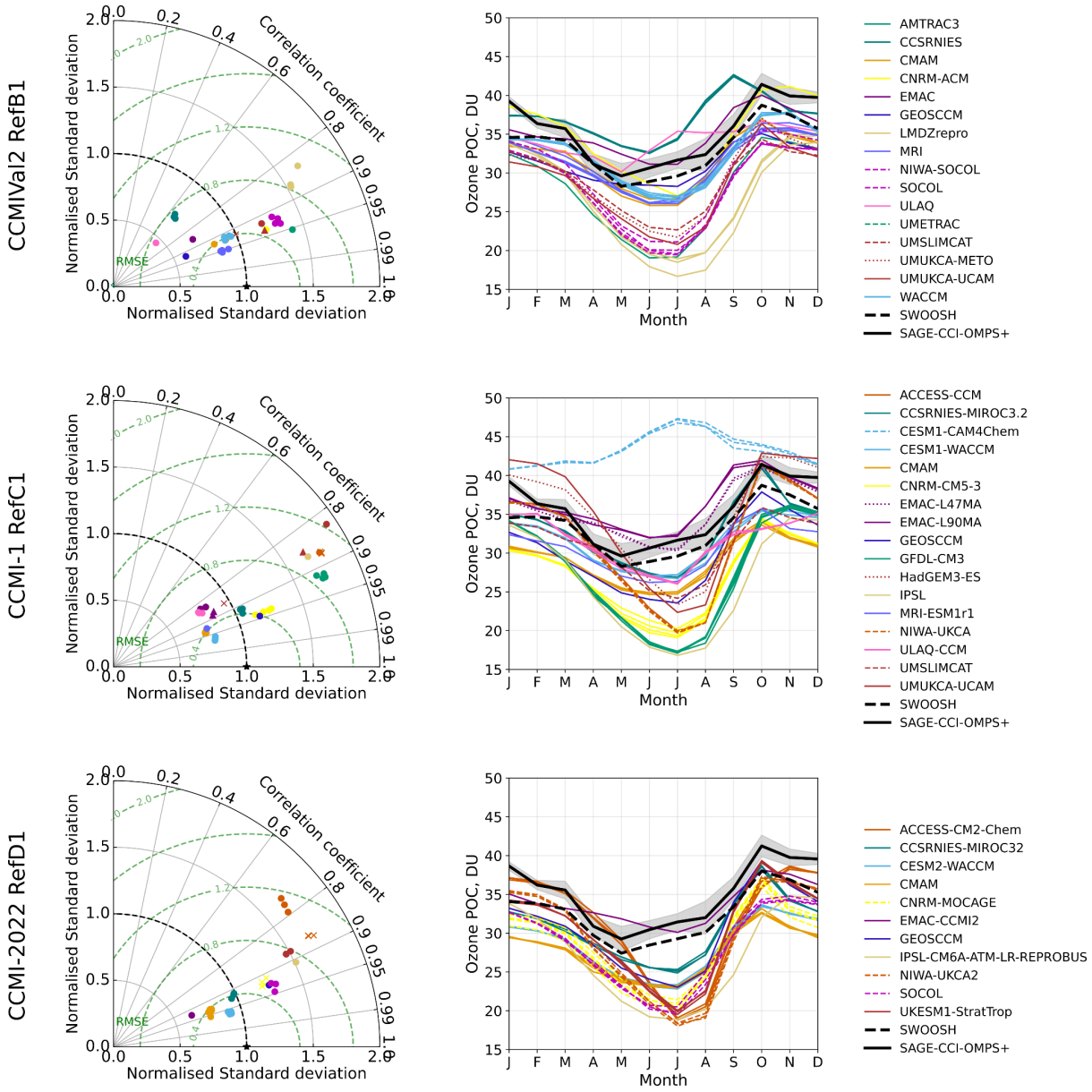

Figure 32S. Ozone partial column in the upper stratosphere for the SH polar region (90S-60S) for individual models participating in the three intercomparison initiatives. Left panels: Taylor diagrams. Right panels: seasonal cycle.

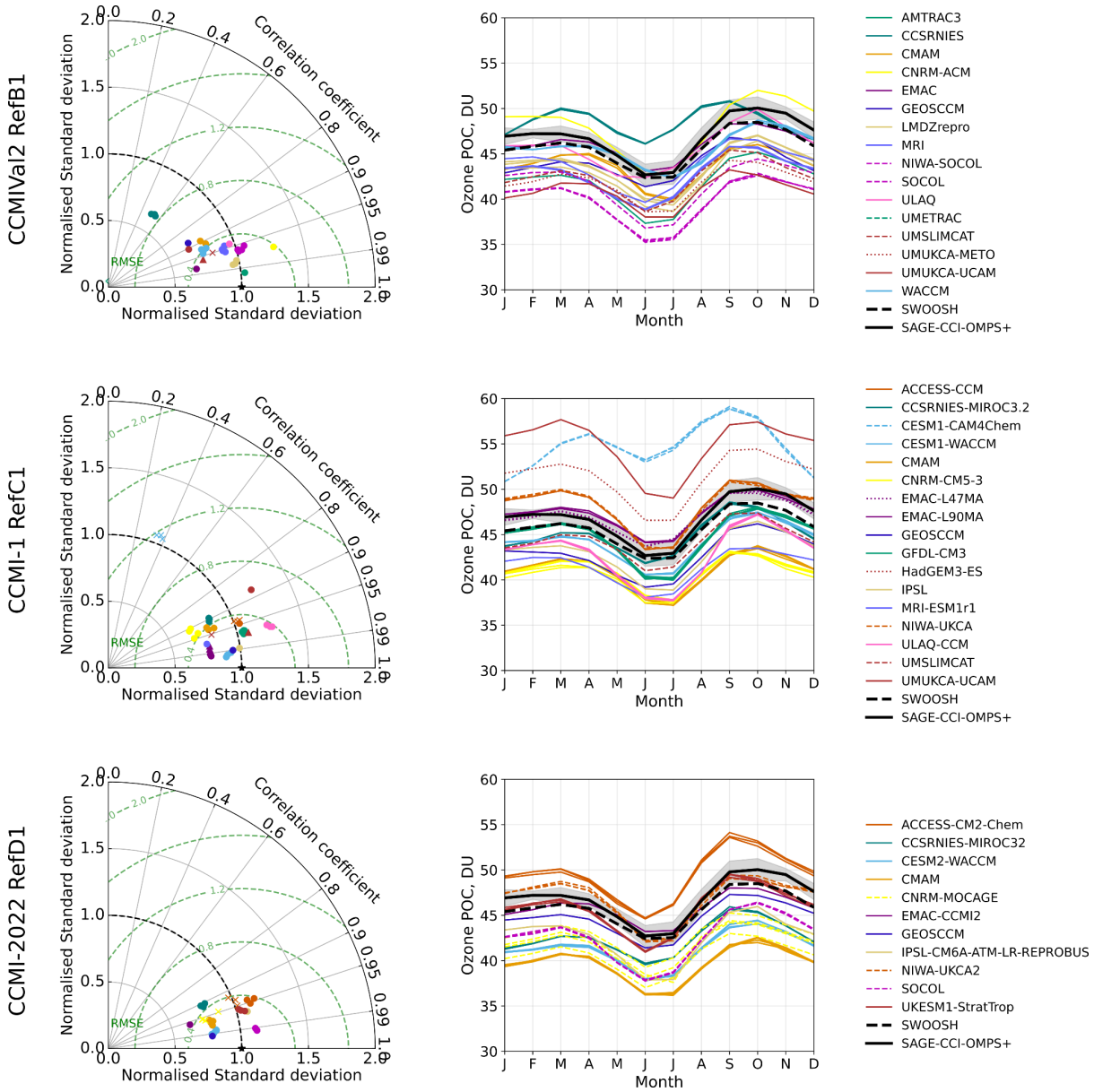

Figure 33S. Ozone partial column in the upper stratosphere for the SH midlatitudes region (60S-30S) for individual models participating in the three intercomparison initiatives. Left panels: Taylor diagrams. Right panels: seasonal cycle.

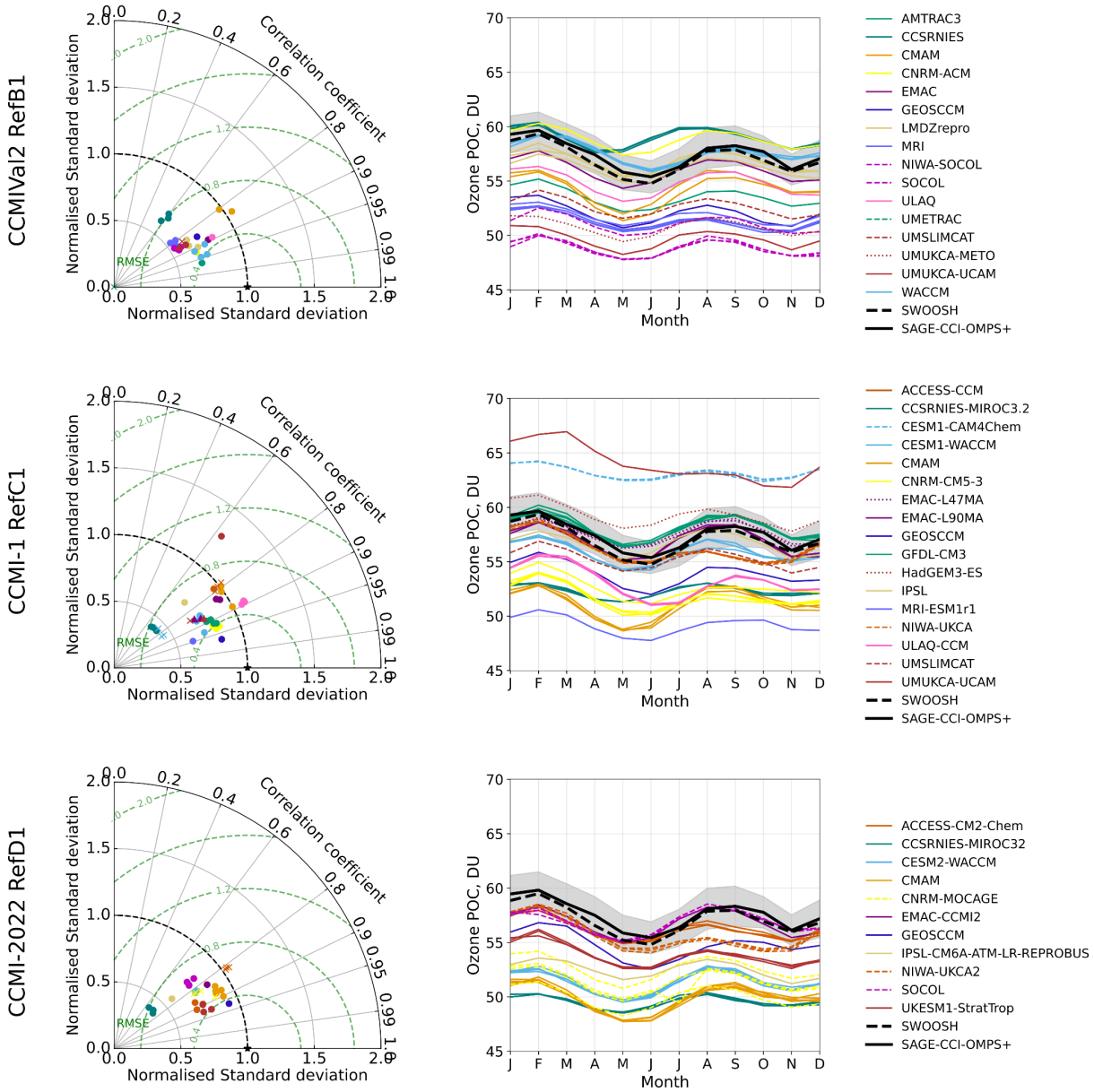

Figure 34S. Ozone partial column in the upper stratosphere for the tropics region (20S-20S) for individual models participating in the three intercomparison initiatives. Left panels: Taylor diagrams. Right panels: seasonal cycle.

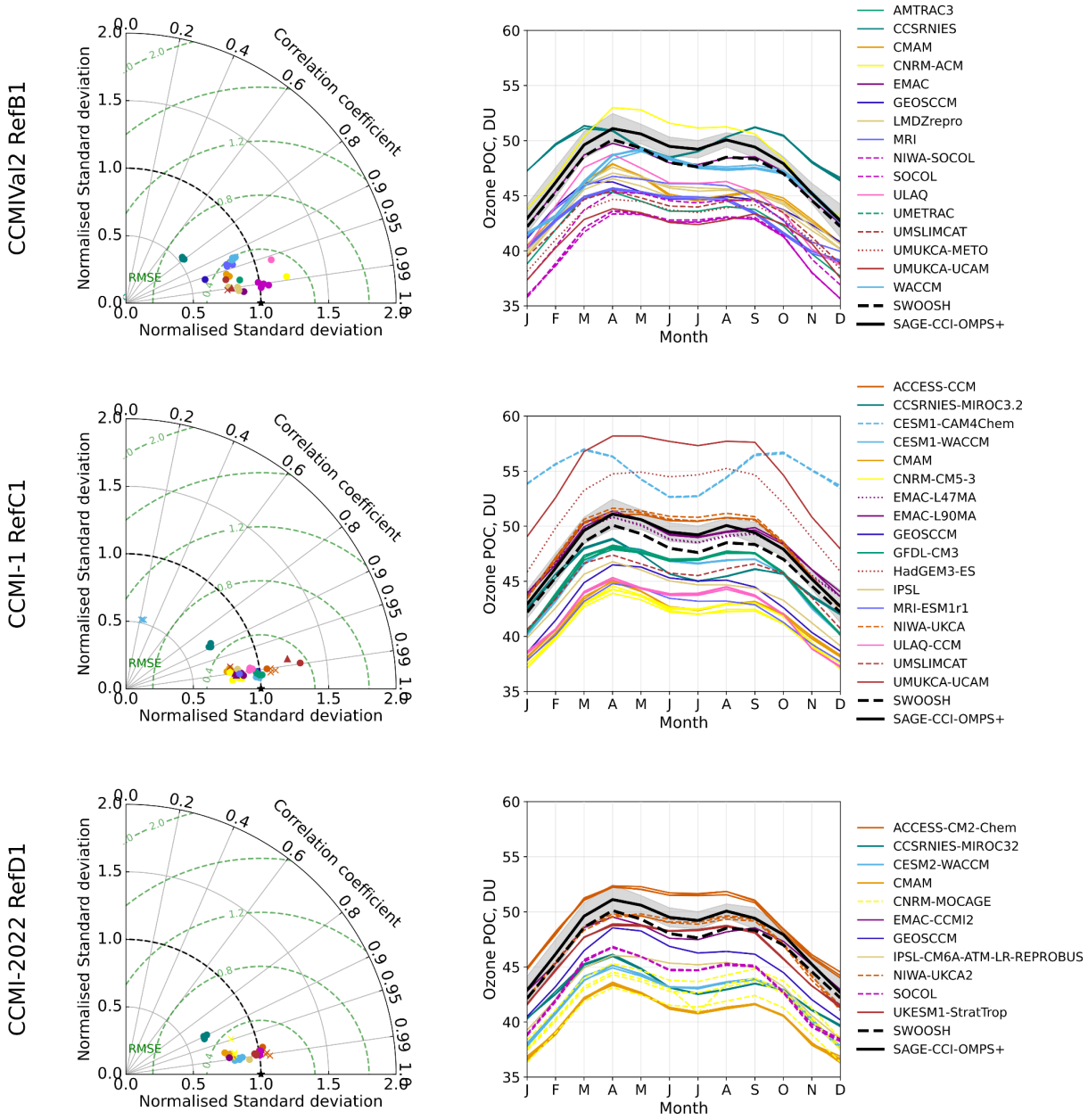

Figure 35S. Ozone partial column in the upper stratosphere for the NH midlatitudes region (30N-60N) for individual models participating in the three intercomparison initiatives. Left panels: Taylor diagrams. Right panels: seasonal cycle.

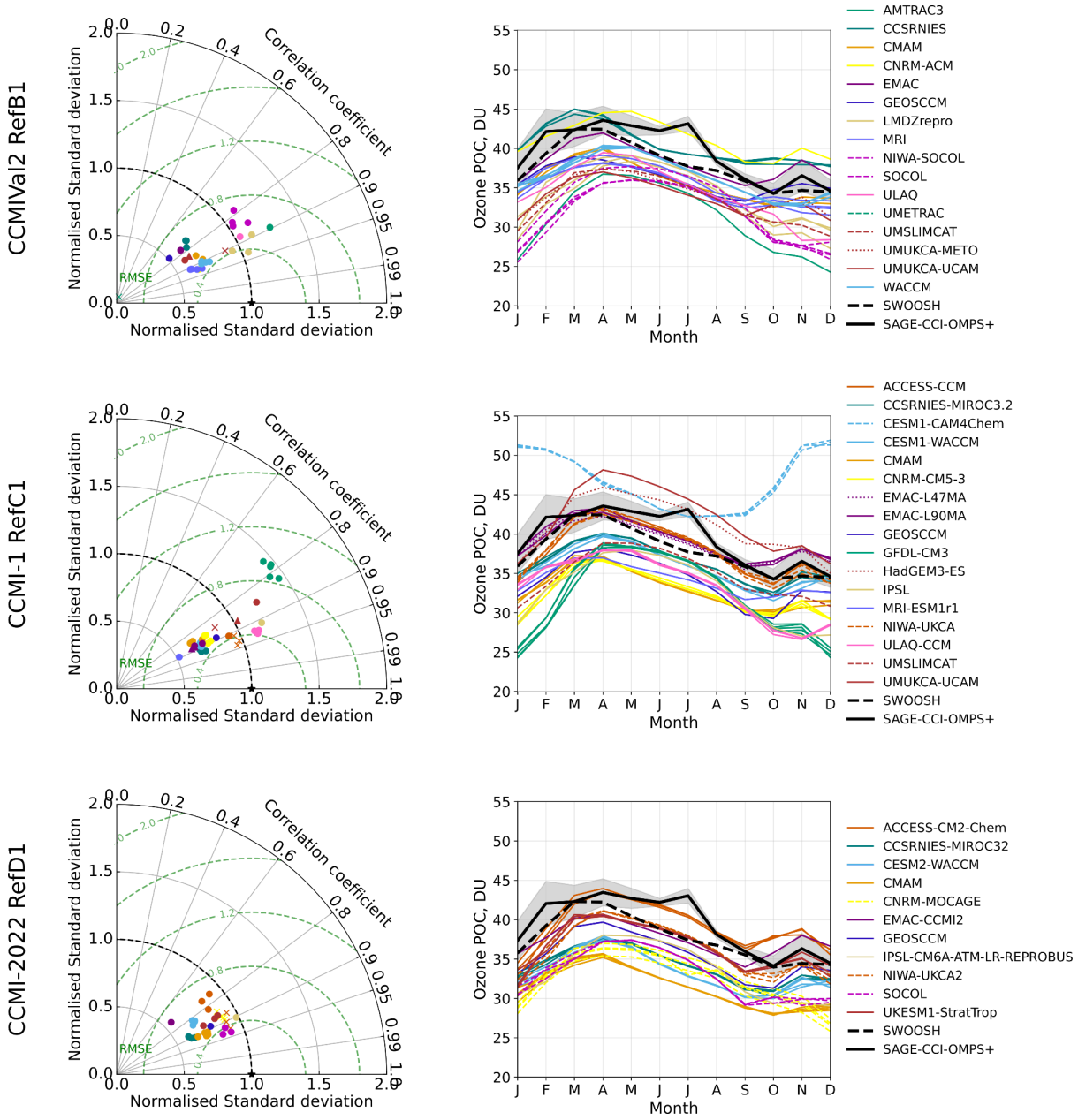

Figure 36S. Ozone partial column in the upper stratosphere for the NH polar region (60N-90N) for individual models participating in the three intercomparison initiatives. Left panels: Taylor diagrams. Right panels: seasonal cycle.

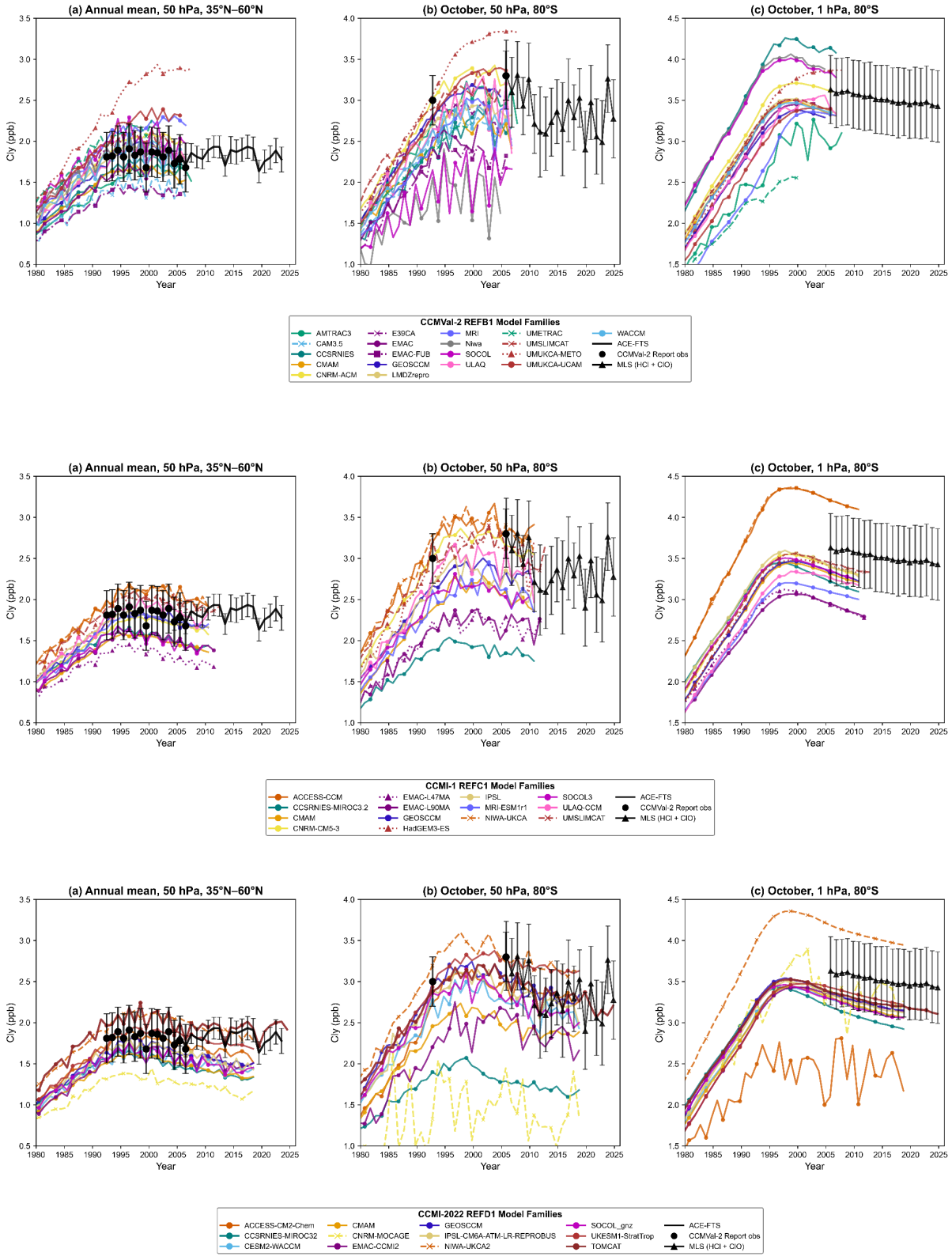

Figure 37S. Timeseries of Cly in individual models participating in the three intercomparison initiatives. All models are shown, while in the main manuscript median plots the following models are removed: CCMVal-2 refB1: UMUKCA-METO, AMTRAC3, UMETRAC; CCMI-1 refC1: NIWA-UKCA, ACCESS-CCM; CCMI-2022 refD1: CNRM-MOCAGE, ACCESS-CM2-Chem, NIWA-UKCA2.

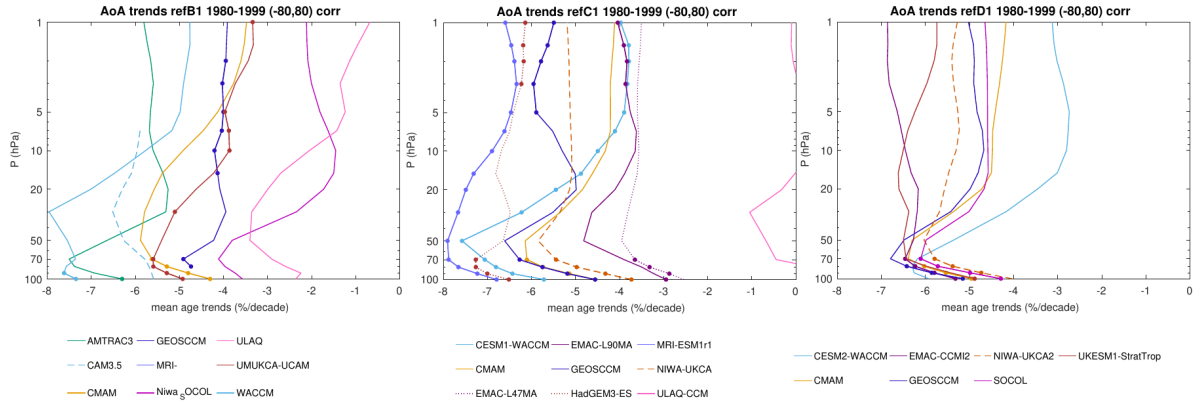

Figure 38S. Trends in mean age of air in individual models participating in the three intercomparison initiatives.

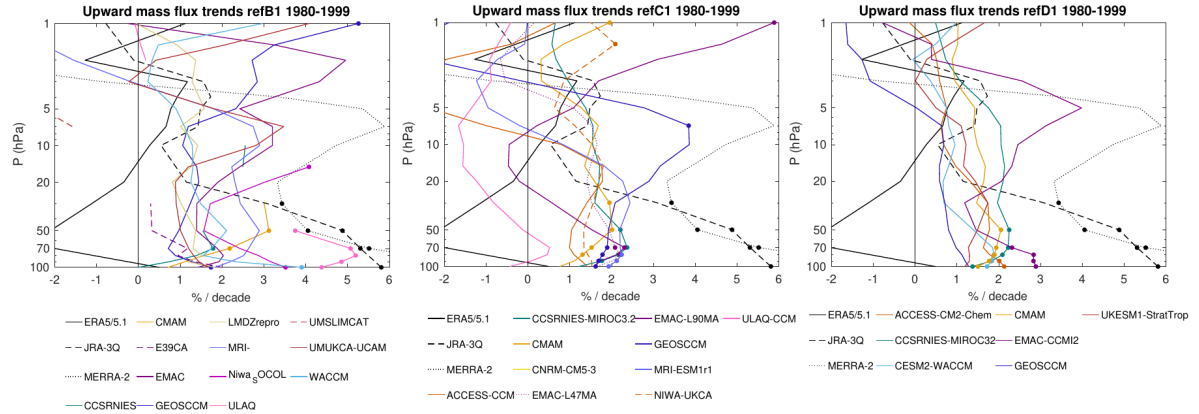

Figure 39S. Trends in upward mass flux in individual models participating in the three intercomparison initiatives.

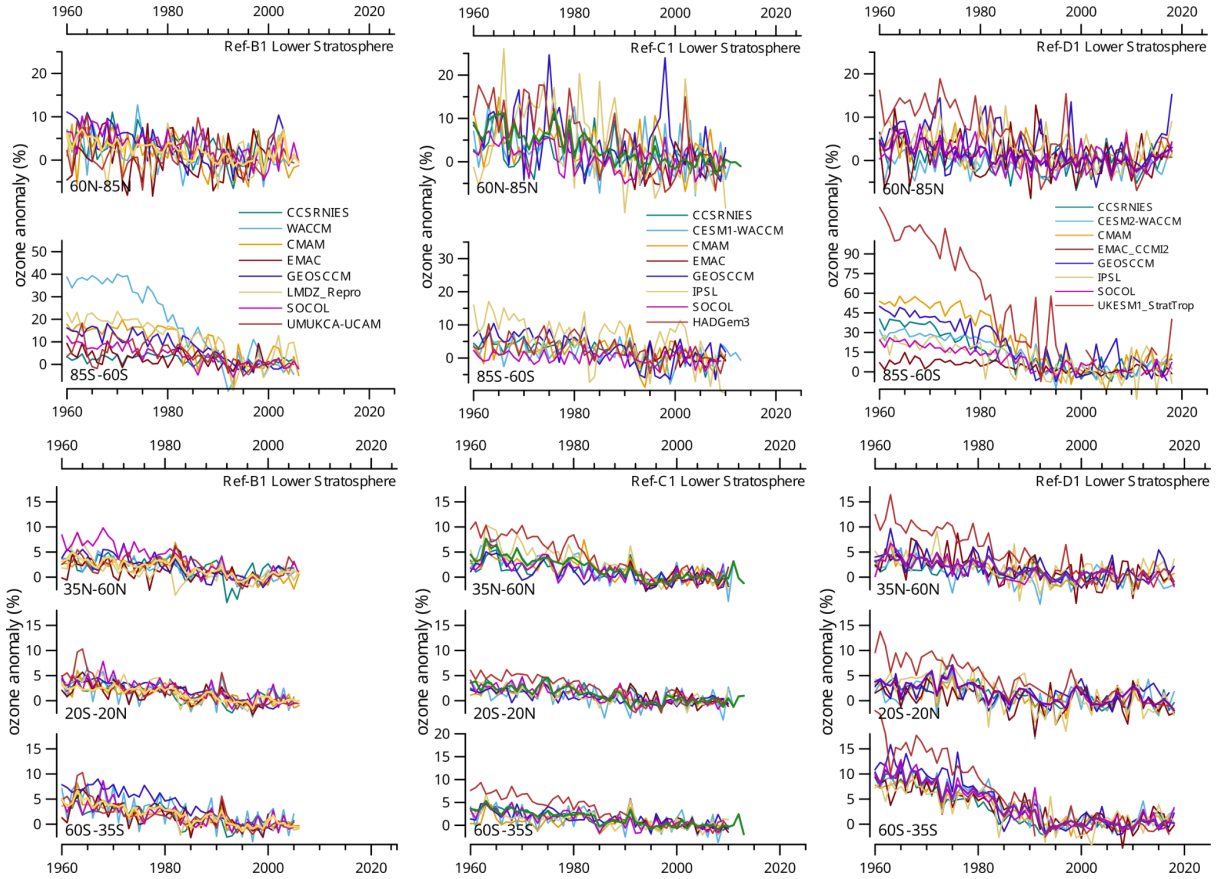

Figure 40S. Timeseries of ozone partial column anomalies for the lower stratosphere in individual models participating in the three intercomparison initiatives.

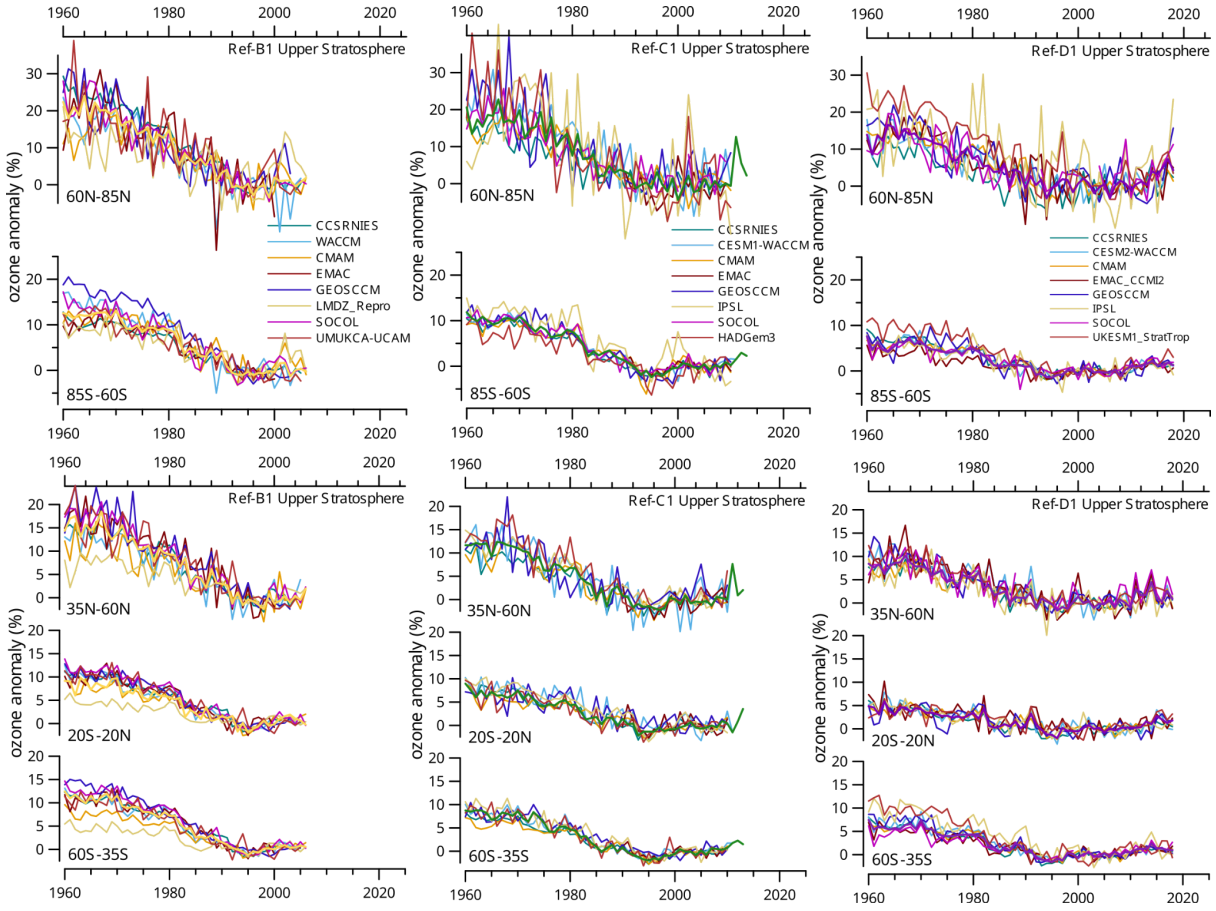

Figure 41S. Timeseries of ozone partial column anomalies for the upper stratosphere in individual models participating in the three intercomparison initiatives.